

Elsevier Editorial System(tm) for Geomorphology
Manuscript Draft

Manuscript Number:

Title: Glacial geomorphology of terrestrial-terminating fast flow lobes/ice stream margins in the southwest Laurentide Ice Sheet

Article Type: Research Paper

Keywords: Terrestrial-terminating ice stream; Push moraines; Hummocky terrain; Glacitectonic thrusting; Controlled moraine; Thermal regime; Laurentide Ice Sheet; Palaeoglaciology

Corresponding Author: Dr. David Evans,

Corresponding Author's Institution: University of Durham

First Author: David Evans

Order of Authors: David Evans; David J Evans; Nathaniel J Young; Colm O Cofaigh

Abstract: Glacial geomorphological mapping of southern Alberta, Canada reveals landform assemblages that are diagnostic of terrestrial-terminating ice stream margins with lobate snouts. Spatial variability in the features that comprise the landform assemblages reflects changes in palaeo-ice stream activity and snout basal thermal regimes. Such changes are potentially linked to regional climate controls at the southwest margin of the Laurentide Ice Sheet. Palaeo-ice stream tracks reveal distinct inset sequences of fan-shaped flow sets indicative of receding lobate ice stream margins. These margins are demarcated by: a) large, often glacially overridden transverse moraine ridges, commonly comprising glacitectonically thrust bedrock; and b) smaller, closely spaced recessional push moraines and hummocky moraine arcs. The former southern margins of the Central Alberta Ice Stream constructed a complex glacial geomorphology comprising minor transverse ridges (MTR types 1-3), hummocky terrain (Types 1-3), flutings and meltwater channels/spillways. MTR Type 1 ridges likely originated through glacitectonic thrusting and have been glacial overrun and moderately streamlined. MTR Type 2 sequences are recessional push moraines similar to those developing at modern active temperate glacier snouts. MTR Type 3 ridges document moraine construction by incremental stagnation, because they occur in association with hummocky terrain. The close association of hummocky terrain with push moraine assemblages, indicates that they are the products of supraglacial controlled deposition on a polythermal ice sheet margin, where the Type 3 hummocks represent former ice-walled lake plains. The ice sheet marginal thermal regime switches indicated by the spatially variable landform assemblages in southern Alberta are consistent with palaeoglaciological reconstructions proposed for other ice stream lobate margins of the southern Laurentide Ice Sheet, where alternate cold, polythermal and temperate marginal conditions sequentially gave way to more dynamic and surging activity.

Suggested Reviewers: Nigel Atkinson

nigel.atkinson@ercb.ca

Works on the Quaternary glacial geology of Alberta and knows the region extremely well.

Rod Smith

Rod.Smith@NRCan-RNCan.gc.ca

Works at the GSC office in Calgary and knows the glacial history of the region very well.

Lionel Jackson

Lionel.Jackson@NRCan-RNCan.gc.ca

Worked all his career on the glacial landforms of western Canada and knows the region intimately.

Art Dyke

Art.Dyke@NRCan-RNCan.gc.ca

Has worked extensively on polythermal ice sheet margins and understands the palaeoglaciological implications of our paper.

Glacial geomorphology of terrestrial-terminating fast flow lobes/ice stream margins in the southwest Laurentide Ice Sheet

David J.A. Evans, Nathaniel J.P. Young and Colm Ó Cofaigh

Highlights

1. Landform assemblages indicative of terrestrial-terminating palaeo-ice streams.
2. Spatial variability in landforms reflects changing palaeo-ice stream thermal regime.
3. Hummocky terrain and push moraine associations indicate polythermal snouts.
4. Receding ice margins alternated between cold, polythermal and temperate conditions.

1 **Glacial geomorphology of terrestrial-terminating fast flow lobes/ice**
2 **stream margins in the southwest Laurentide Ice Sheet**

3

4 David J.A. Evans, Nathaniel J.P. Young and Colm Ó Cofaigh

5 Department of Geography, Durham University, South Road, Durham, DH1 3LE, UK

6

7 **Abstract**

8 Glacial geomorphological mapping of southern Alberta, Canada reveals landform assemblages
9 that are diagnostic of terrestrial-terminating ice stream margins with lobate snouts. Spatial
10 variability in the features that comprise the landform assemblages reflects changes in palaeo-ice
11 stream activity and snout basal thermal regimes. Such changes are potentially linked to regional
12 climate controls at the southwest margin of the Laurentide Ice Sheet. Palaeo-ice stream tracks
13 reveal distinct inset sequences of fan-shaped flow sets indicative of receding lobate ice stream
14 margins. These margins are demarcated by: a) large, often glacially overridden transverse
15 moraine ridges, commonly comprising glacitectonically thrust bedrock; and b) smaller, closely
16 spaced recessional push moraines and hummocky moraine arcs. The former southern margins of
17 the Central Alberta Ice Stream constructed a complex glacial geomorphology comprising minor
18 transverse ridges (MTR types 1-3), hummocky terrain (Types 1-3), flutings and meltwater
19 channels/spillways. MTR Type 1 ridges likely originated through glacitectonic thrusting and
20 have been glacial overrun and moderately streamlined. MTR Type 2 sequences are recessional
21 push moraines similar to those developing at modern active temperate glacier snouts. MTR
22 Type 3 ridges document moraine construction by incremental stagnation, because they occur in
23 association with hummocky terrain. The close association of hummocky terrain with push
24 moraine assemblages, indicates that they are the products of supraglacial controlled deposition
25 on a polythermal ice sheet margin, where the Type 3 hummocks represent former ice-walled
26 lake plains. The ice sheet marginal thermal regime switches indicated by the spatially variable
27 landform assemblages in southern Alberta are consistent with palaeoglaciological
28 reconstructions proposed for other ice stream lobate margins of the southern Laurentide Ice

29 Sheet, where alternate cold, polythermal and temperate marginal conditions sequentially gave
30 way to more dynamic and surging activity.

31

32 **Key words:** terrestrial-terminating ice stream; push moraines; hummocky terrain; glacitectonic
33 thrusting; controlled moraine; thermal regime; Laurentide Ice Sheet; palaeoglaciology

34

35 **1. Introduction and rationale**

36 The important role of ice streams in ice sheet dynamics has resulted in them becoming
37 increasingly more prominent as a focus of multi-disciplinary research in process glaciology and
38 palaeoglaciology. Ongoing research questions surround the issues of maintenance and
39 regulation of ice flow, temporal and spatial patterns of activation/deactivation, large scale
40 changes in flow regime, and potential linkages/responses to climate. Some insights into these
41 questions are emerging from the studies of former ice sheet beds, but the focus of such research
42 has been largely targeted at marine-terminating ice streams. Details on the marginal activity of
43 terrestrially-terminating ice streams has only recently emerged from the study of the former ice
44 streams of the southern Laurentide Ice Sheet, where it is clear that ice stream margins
45 constructed lobate assemblages of moraines during deglaciation (Patterson 1997, 1998; Jennings
46 2006; Evans et al. 2008, 2012; Ó Cofaigh et al. 2010).

47

48 The western plains of southern Alberta, southwest Saskatchewan and northern Montana contain
49 a wealth of glacial landforms that has been previously widely employed in reconstructions of
50 Laurentide Ice Sheet palaeoglaciology (Stalker 1956, 1977; Christiansen 1979; Clayton &
51 Moran 1982; Clayton et al. 1985; Evans & Campbell 1992, 1995; Evans 2000; Evans et al.
52 1999, 2006, 2008, 2012; Ó Cofaigh et al. 2010), while at the same time being central to
53 conceptual developments in glacial geomorphology (e.g. Gravenor & Kupsch 1959; Stalker
54 1960, 1973, 1976; Clayton & Cherry 1967; Bik 1969; Clayton & Moran 1974; Moran et al.
55 1980; Kehew & Lord 1986; Tsui et al. 1989; Beaty 1990; Alley 1991; Evans 1996, 2003, 2009;
56 Eyles et al. 1999; Mollard 2000; Boone & Eyles 2001; Clayton et al. 2008). Significant debate

57 has also been recently centred on alternative, subglacial megaflood interpretations of the
58 landforms of the region (cf. Rains et al. 1993, 2002; Sjogren & Rains 1995; Shaw et al. 1996;
59 Munro-Stasiuk & Shaw 1997, 2002; Munro-Stasiuk 1999; Beaney & Hicks 2000; Beaney &
60 Shaw 2000; Beaney 2002; Shaw 2002, 2010; Clarke et al. 2005; Benn & Evans 2006; Evans et
61 al. 2006; Evans 2010). Notwithstanding the volume of publications in support of a subglacial
62 megaflood origin for much of the glacial geomorphology of the region, we here provide a
63 landsystems approach to the interpretation of the glaciation legacy as it pertains to the Late
64 Wisconsinan advance and retreat of the southwest Laurentide Ice Sheet in the context of the
65 palaeo-ice stream activity demonstrated by Shetsen (1984), Evans et al. (1999; 2006, 2008,
66 2012), Evans (2000) and Ó Cofaigh et al. (2010). This approach makes the assumption at the
67 outset that subglacially streamlined bedforms and ice-flow transverse landforms are not the
68 product of megafloods, an assumption soundly based in the arguments presented in a number of
69 carefully reasoned ripostes (Clarke et al. 2005; Benn & Evans 2006; Evans et al. 2006) to the
70 megaflood hypothesis. The latter have demonstrated that the western plains contain an
71 invaluable record of palaeo-ice stream activity pertaining to the dynamics of terrestrially-
72 terminating systems, wherein spatial and temporal patterns of ice stream operation within an ice
73 sheet are recorded in the regional glacial geomorphology. This forms a contrast to the vertical
74 successions of marine sediments that record the activity of marine-terminating ice streams in
75 offshore depo-centres such as trough-mouth fans.

76

77 The overall aim of this research is to augment recent developments of the till sedimentology and
78 stratigraphy of the western Laurentide Ice Sheet palaeo-ice stream imprints (Evans et al. 2012)
79 with investigations of the landform signature of these terrestrially-terminating systems in
80 southern Alberta (Fig. 1). This in turn facilitates the evaluation and reconstruction of the
81 marginal dynamics of terrestrial palaeo-ice streams in the wider context. Specific objectives
82 include: 1) the use of SRTM and Landsat ETM+ imagery and aerial photographs to map the
83 glacial geomorphology of southern Alberta, with particular focus on the impact of the palaeo-ice
84 streams/lobes proposed by Evans et al. (2008); and 2) the identification of diagnostic landforms

85 or landform assemblages (landsystems model) indicative of terrestrial-terminating ice stream
86 margins and an assessment of their implications for reconstructing palaeo-ice stream dynamics.

87

88 **2. Study area and previous research**

89 The study area is located in the North America Interior Plains, specifically in the southern part
90 of the province of Alberta in western Canada, between longitudes 110°-114°W and latitudes
91 49°-52°N. It is bordered by the Rocky Mountain Foothills in the west, the Tertiary gravel-
92 topped monadnocks of the Cypress Hills in the southeast and Milk River Ridge to the south
93 (Fig. 1; Leckie 2006)). Geologically, the southern Alberta plains lie within the Western
94 Canadian Sedimentary Basin, on a northerly dipping anticline known as the Sweet Grass Arch
95 (Westgate, 1968). The Interior Plains in this area are composed of Upper Cretaceous and
96 Tertiary sediments, which consist of poorly consolidated clay, silt and sand (Stalker, 1960;
97 Klassen, 1989; Beaty, 1990). The preglacial and interglacial landscapes were dominated by
98 rivers flowing to the north and northeast and which repeatedly infilled and re-incised numerous
99 pre-glacial and interglacial valleys, with sediments ranging in age from late Tertiary/Early
100 Quaternary (Empress Group) to Wisconsinan (Stalker 1968; Evans & Campbell, 1995). The
101 Cypress Hills and Del Bonita Highlands of the Milk River Ridge formed nunataks during
102 Quaternary glaciations (Klassen, 1989).

103

104 The striking glacial geomorphology of Alberta was primarily formed during the Late
105 Wisconsinan by ice lobes/streams flowing from the Keewatin sector of the Laurentide Ice Sheet,
106 which coalesced with the Cordilleran Ice Sheet over the high plains to form a southerly flowing
107 suture zone marked by the Foothills Erratics Train (Stalker, 1956; Jackson et al., 1997, 2011;
108 Rains et al., 1999; Dyke et al. 2002; Jackson & Little 2004). At its maximum during the late
109 Wisconsinan, the ice flowed through Alberta and into northern Montana (Colton et al., 1961;
110 Westgate, 1968; Colton and Fullerton, 1986; Dyke and Prest, 1987; Fulton, 1995; Kulig, 1996;
111 Dyke et al., 2002; Fullerton et al., 2004a, b; Davies et al., 2006). Ice sheet reconstructions
112 suggest that deglaciation from Montana started c.14 ka BP, and had retreated to the “Lethbridge

113 moraine” by c.12.3 ka BP, after which it receded rapidly to the north (Stalker 1977; Clayton and
114 Moran, 1982; Dyke and Prest, 1987).

115

116 Mapping of the glacial geomorphology of southern and central Alberta (Stalker, 1960; 1977;
117 Prest et al., 1968; Westgate, 1968; Shetsen, 1987, 1990; Fulton, 1995, Evans et al., 1999, 2006,
118 2008) has enabled a broad identification of ice flow patterns and ice-marginal landform
119 assemblages. Three prominent fast flowing ice lobes appear to have operated within the region
120 and were identified as the “east”, “central” and “west lobes” by Shetsen (1984) and Evans
121 (2000). Recently, Evans et al. (2008) suggested that the west and central lobes be referred to as
122 the High Plains Ice Stream (HPIS) and Central Alberta Ice Stream (CAIS) respectively due to
123 their connection to corridors of highly streamlined terrain which are interpreted as the imprint of
124 trunk zones of fast ice flow (Fig. 1b). The CAIS has also been referred to as the “Lethbridge
125 lobe” by Eyles et al. (1999), who highlighted that its margins were defined by the McGregor,
126 Lethbridge and Suffield moraine belts. These moraine belts comprise landforms of various
127 glacial origins, including thrust moraines, (Westgate, 1968; Stalker, 1973, 1976; Tsui et al.,
128 1989; Evans, 1996, 2000; Evans & Rea, 2003; Evans et al., 2008), “hummocky terrain” (cf.
129 Gravenor & Kupsch, 1959; Stalker, 1960; 1977; Shetsen, 1984, 1987, 1990; Clark et al., 1996;
130 Munro-Stasiuk & Shaw, 1997; Evans et al., 1999, 2006; Evans 2003; Eyles et al. 1999; Boone
131 & Eyles 2001; Johnson & Clayton 2003; Munro-Stasiuk & Sjogren, 2006) and recessional push
132 moraines and/or controlled moraine (Evans et al. 1999, 2006, 2008; Evans 2003; Johnson &
133 Clayton 2003). Glacially overridden and streamlined moraines also appear in the trunk zones of
134 the fast glacier flow tracks (Evans et al. 2008), although their origins and ages remain to be
135 elucidated. Localized case studies of large scale moraine mapping by Evans et al. (1999, 2006,
136 2008) have identified a spatial variability that potentially reflects changing thermal regimes at
137 the sheet margin in addition to surging activity during later stages of recession, similar to the
138 trends identified by Colgan et al. (2003) in the northern USA.

139

140 During deglaciation of the region, numerous proglacial lakes developed in front of the receding
141 lobate ice stream margins, resulting in the incision of numerous spillways (Christiansen 1979;

142 Evans, 2000). These spillways have been either cut through pre-existing preglacial valley fills or
143 have created new flood tracks through the soft Cretaceous bedrock (Evans & Campbell 1995).
144 As meltwaters decanted generally eastwards, they appear to have penetrated beneath the ice
145 sheet margin in some places to produce subglacial meltwater channels (Sjogren & Rains 1995).
146 This pattern of drainage was most likely enhanced by the northeasterly dip in the
147 glacioisostatically depressed land surface beneath the receding ice sheet, although regional
148 isobases have not been reconstructed for this region due to the lack of datable lake shorelines.

149

150 A complex stratigraphy of pre-Quaternary and Quaternary glacial and interglacial deposits
151 exists in the study region (Stalker 1963, 1968, 1969, 1983; Stalker & Wyder 1983; Evans &
152 Campbell 1992, 1995; Evans 2000). Of significance to this study are the extensive outcrops of
153 glacial sediment relating to the last glaciation, which have been employed in
154 palaeoglaciological reconstructions of ice streams and ice sheet marginal recession patterns by
155 Evans (2000), Evans et al. (2006, 2008, 2012) and Ó Cofaigh et al. (2010; Fig. 1c). These
156 studies have highlighted the marginal thickening of subglacial traction tills in association with
157 individual ice streams/lobes, thereby verifying theoretical models of subglacial deforming layers
158 (e.g. Boulton 1996a, b) beneath ice sheets.

159 The findings of the research reviewed above are assimilated in this study with new observations
160 and data on the glacial landforms of the region in order to assess the regional imprint of ice
161 stream marginal sedimentation. Local variations in the landform patterns in turn facilitate a
162 better understanding of ice stream dynamics during the deglaciation of western Canada.

163 **3. Methods**

164 Glacial geomorphological mapping was undertaken by using three different aerial image
165 sources, including the 2000 Shuttle Radar Topography Mission (SRTM), Landsat 7 Enhanced
166 Thematic Mapper Plus (Landsat ETM+) and aerial photograph mosaics flown and compiled by
167 the Alberta Government in the 1950s. The SRTM data have been used to create digital elevation
168 models (DEMs) of the Alberta landscape. Several authors (e.g. Glasser & Jansson, 2005; Bolch

169 et al., 2005; Heyman et al., 2008) have used SRTM data for mapping geomorphology, but have
170 all used it in conjunction with another data set such as Landsat 7 ETM+ and ASTER, because
171 its resolution is not regarded as optimum for mapping exercises. Smith et al. (2006) have
172 suggested that spaceborne sensors such as SRTM are not sensitive enough to map detailed
173 morphology. Similarly, Falorni et al. (2005) have commented on a link between high
174 topography and vertical accuracy errors within SRTM data sets. This implies that SRTM
175 imagery will provide a good regional scale picture, yet where landforms exist at scales smaller
176 than, or approaching, pixel resolution it is likely that they will not be visible, resulting in a
177 generalized rather than a comprehensive map of the glacial geomorphology. Nonetheless, Ó
178 Cofaigh et al. (2010) have used solely SRTM data to map ice streams in Saskatchewan and
179 Alberta, yielding fine resolution details of subglacial bedforms and marginal moraines.

180 Global Mapper™ produced a smoothed, rendered pseudo-colour image of the SRTM data that
181 could be manipulated to accentuate features, produce 3D images and change sun illumination
182 angles. By vertically stretching the elevation data, it is possible to more easily identify
183 landforms within the data set, providing that the exaggeration of morphology is acknowledged.
184 Following the procedures of Smith and Clark (2005), multiple illumination angles were also
185 used during mapping. The Global Mapper™ interface does not provide the ability to easily map
186 the glacial geomorphology and so these manipulations were completed in Global Mapper and
187 then exported as a GeoTIFF. Because GeoTIFFs provide only georeferenced raster imagery
188 with no topographic information, the DEM manipulations were processed prior to GeoTIFF
189 creation. The images were then opened in Erdas Imagine 9.0, a GIS package that enables easy
190 mapping of the glacial landforms. In order to map these features, vector layers were created and
191 placed on top of the exported GeoTIFFs.

192 An alternative method was employed to compare, verify and supplement the SRTM mapping.
193 This involved the use of ENVI 4.3 software to open the SRTM data in a grey scale format;
194 nearest neighbour sampling was used to correct for missing sample points and was
195 automatically applied to the same missing data points when opening the images in Global
196 Mapper. The files were then exported from ENVI as Bitmap Graphic files ‘.img’, which are

197 simply raster files that can carry both georeferenced and topographic information. This option
198 was not available when exporting out of Global Mapper. These images were opened in Erdas
199 Imagine 9.0 as relief shaded DEMs. The DEMs were manipulated in exactly the same manner
200 as above, with sun illumination changes, vertical exaggeration and 3D profiling. In similar
201 fashion to the above method, vector files were overlaid on the DEMs to map the landforms. The
202 results were then compared to the mapping performed from the GeoTIFFs.

203 Additional geomorphological mapping was conducted through interpretation of the high
204 resolution Landsat ETM+ panchromatic band (band 8: 0.52-0.90 μm) images. A mosaic of 13
205 scenes provided full coverage of the field site. These were downloaded from the GeoBase
206 website (<http://www.geobase.ca/geobase/en/index.html>) overseen by the Canadian Council on
207 Geomatics (CCOG). All images were in GeoTIFF format, and were georeferenced with the
208 North American datum of 1983 (NAD83), corresponding to the Universal Transverse Mercator
209 (UTM) projection, UTM Zone 12 for Alberta. The images were opened in Erdas Imagine 9.0
210 and overlaid with the same vector layers that were used to map the DEMs. This allowed first
211 order verification of the SRTM interpretations and the mapping of additional features.

212 The SRTM and Landsat ETM+ mapping is at a scale appropriate to the identification of regional
213 scale landform patterns, including subglacial bedform flowsets and cross-cutting lineations
214 (Clark 1999). Once identified, flowsets were mapped by drawing flowlines orientated parallel to
215 the lineation direction. Where possible, quantitative analyses examined average lineation length,
216 orientation, elongation ratios (ER) and average distance between lineations, in order to identify
217 any similarities or differences between flowsets. Such quantitative analyses of subglacial
218 bedforms have been widely demonstrated to be critical in the reconstruction of palaeo-ice
219 streams and their dynamics (e.g. Stokes & Clark, 2003a; Roberts & Long, 2005; Stokes et al.,
220 2006; Storrar & Stokes, 2007).

221 Aerial photograph mosaics were utilized for large scale investigations into the landform record
222 of the southern Alberta ice stream margins, specifically because the remote sensing methods did
223 not have sufficient resolution. A series of ten, 1:63,360 (1 inch to one mile) aerial photograph
224 mosaics captured in 1951 by the Alberta Department of Land and Forests were utilized for the

225 mapping of landforms associated with the recession of the Laurentide Ice Sheet margin,
226 especially the CAIS of Evans et al. (2008), in southern Alberta. Landforms were mapped
227 according to their morphometric characteristics prior to interpretation, although genetic terms
228 were later used to identify features on the maps. Linear depositional features, both ice flow-
229 parallel (flutings, eskers) and ice flow-transverse (major and minor ridges or moraines) were
230 mapped as single lines representing their summit crests. In areas of “hummocky terrain” (*sensu*
231 Benn & Evans 2010), the complexity and density of individual hummocks rendered the
232 mapping of every mound inappropriate and hence the hummocky terrain is represented by black
233 shading of the inter hummock depressions. This approach effectively illustrates the relative
234 degrees of linear versus chaotic patterns.

235 **4. Results of geomorphological mapping**

236 **4.1 Regional palaeo-ice stream geomorphology: small scale mapping case studies of the** 237 **HPIS and CAIS tracks**

238 The glacial geomorphology of southern Alberta is dominated by the imprints of two fast ice
239 flow or palaeo-ice stream tracks, which appear as corridors of smoothed topography (the HPIS
240 and CAIS of Evans et al., 2008) bordered by lobate marginal landforms and inter-lobate/inter-
241 stream hummocky terrain. Also, in the eastern part of the province, the subglacial bedforms and
242 marginal moraines of Ó Cofaigh et als. (2010) 'Ice Stream 1' (“east lobe” of Shetsen 1984 &
243 Evans 2000) terminate on the north slopes of the Cypress Hills. Previous work on regional
244 mapping in Alberta by Evans et al. (2008) identified the fast flow tracks and various ice-flow
245 transverse ridges, some of which were difficult to interpret due to the low resolution of the
246 DEMs available at the time. Here we report on the comprehensive and systematic mapping and
247 quantification of landforms in the HPIS and CAIS tracks (Figs. 1 & 2) based on higher
248 resolution SRTM data and further developing the mapping of Ó Cofaigh et al. (2010; Fig. 1c).

249

250 The study area contains approximately 250 km of the total length of the HPIS (see Evans et al.
251 2008 for details of entire ice stream track) and its width varies from around 50 km along the
252 main trunk to 85 km across the lobate terminus. A total of 714 lineations were identified along

253 the CAIS and HPIS and together comprise seven individual flow-sets, although large areas of
254 the smoothed corridors that demarcate the fast flow trunks do not contain terrain sufficiently
255 strongly fluted to enable confident flowset mapping (Fig. 3). The main landforms in the HPIS
256 trunk include at least five (Hfs_1-5) different flow sets (Fig. 3), four of which (Hfs_2-5) record
257 marginal splaying or lobate flow within the HPIS towards the McGregor Moraine belt. The
258 study area contains approximately 320 km of the total length of the CAIS, over which distance
259 its width increases from 97 km to 160 km at its lobate margin (Figs. 2 & 3). One flow set
260 (CAfs_1) was identified along the CAIS trunk, and one (CAfs_2) in its southeast corner (Fig.
261 3), each flow set relating to different phases of ice stream flow.

262

263 Flow set Hfs_4 contained the largest number of lineations (260) although all flow sets tended to
264 display strong spatial coherency, and CAfs_1 contained the largest lineation at 35km long (cf.
265 Evans 1996). Due to the resolution of SRTM imagery no elongation ratios (ERs) could be taken,
266 however, it is apparent that most lineations have ERs of greater than 10:1. The smallest
267 examples were found in Hfs_1 and the largest in CAfs_1 (see Table 1 for flow set data).

268

269 Flow sets display distinct relationships with ice flow transverse ridges or hummocky terrain
270 arcs, some of which were previously documented at low resolution by Evans et al. (2008).
271 Extensive sequences of transverse ridges exist throughout the study area, not only in marginal
272 settings as sharp crested features but also along the HPIS and CAIS flow corridors as smoothed
273 or streamlined features (Figs. 2, 4-8). These ridges are loosely classified below as minor or
274 major features according to their relative sizes.

275 Transverse ridges associated with the HPIS reveal a clear pattern of ice-marginal advance and
276 recession. For example, flow sets Hfs_4 and 5 terminate in zones of hummocky terrain and/or
277 minor transverse ridges, demarcating lobate ice marginal positions which are compatible with
278 the flow sets that terminate on their proximal sides (cf. Evans et al. 1999, 2006, 2008). The
279 landform assemblage TR_1 occupies approximately 100 km of the western half of the HPIS
280 track and includes an extensive sequence of low amplitude (3-6 m high), inset and arcuate minor

281 transverse ridges (cf. Evans et al. 1999; Evans 2003; Johnson & Clayton 2003). These minor
282 ridges appear to be draped over, or superimposed on two major ridges (Fig. 4). The summits of
283 the two major ridges each comprise up to five component sub-ridges 10-15 m high and are
284 overprinted by flutings, the most prominent relating to flow set Hfs_5 (Fig. 4) which continues
285 in a southeasterly direction to cover the area known as Blackspring Ridge (Munro-Stasiuk &
286 Shaw 2002). A further extensive series of inset arcuate minor ridges (TR_2) lies immediately
287 south of the southernmost major ridge and, together with the TR_1 sequence, has previously
288 been interpreted by Evans et al. (1999) and Evans (2003) as a recessional push moraine
289 sequence.

290 On the CAIS footprint, CAfs_1 terminates north of the largest major transverse ridge in the
291 study area (TR_8; Fig 5) which displays a dual lobate front and is 70 km long and crosses most
292 of the CAIS between the Bow and Oldman Rivers, with its eastern edge connecting to an area of
293 hummocky terrain. The ridge is weakly asymmetric, with a steeper distal slope and its height
294 gradually increases from west to east from 20 to 30 m. The centre of flow set CAfs_1 is
295 connected to TR_8 via an esker complex (Evans 1996, 2000) that joins the ridge at its re-entrant
296 or inflexion point (Figs. 2 & 5). Two sets of minor transverse ridges also occur in the area
297 located between major ridge TR_8 and the southern end of flow set CAfs_1 (Figs. 5 & 6).
298 Assemblage TR_6 comprises broad, shallow ridges superimposed with numerous discontinuous,
299 narrow and sharp ridges (Fig. 6). These have previously been interpreted as glacitectonic thrust
300 ridges by Evans and Campbell (1992) and Evans (2000) based upon field exposures displaying
301 deformed Cretaceous bedrock overlain by till. Assemblage TR_7 includes only the narrow,
302 sharp ridges, which appear to be continuous with those in TR_6 but occupy proglacial/spillway
303 flood tracks previously mapped by Evans (1991, 2000) and therefore have most likely been
304 accentuated by fluvial erosion.

305 Further north in the CAIS footprint, it is apparent that CAfs_1 starts immediately down flow of
306 a streamlined major transverse ridge complex (TR_5; cf. Evans 1996; Evans et al. 2008),
307 comprising three parallel subsets of ridges rising up to 30 m above the surrounding terrain (Fig.
308 8A). In detail the sequence is composed of 40 ridges, ranging from 1-4 km in length and up to 5

309 m high. Other transverse ridges in this area include a cluster of inset minor ridges (TR_3), 30
310 km long and 10 – 20 m high and with crest wavelengths of 500 - 1000 m and bordered by
311 hummocky terrain to the east, west and south. Individual ridges within the sequence are only a
312 few kilometres in length. To the north west of TR_3 are several large ridges set within and
313 dominating an area of hummocky terrain (TR_4). The ridge crests are 10 km long and stand up
314 to 20 m above the surrounding hummocks. These large transverse ridge complexes are strongly
315 asymmetric, with steeper north-facing or proximal slopes.

316 In the extreme south of the study area, on the preglacial drainage divide that was located
317 between the Cypress and Sweet Grass Hills (Westgate, 1968) and 150 m above the Pakowki
318 Lake depression (Fig. 8D), flow set CAfs_2 is located on the down ice side of major ridge
319 assemblage TR_10, whose summit comprises a series of prominent and closely spaced, sharp
320 crested transverse ridges (Fig. 7) which decline in height from 20 to 5 m and wavelength from 1
321 km - 250 m from west to east. The flow set CAfs_2 appears to be superimposed on a small area
322 of ridges in the centre of TR_10, but elsewhere the ridges do not appear streamlined on this
323 imagery. Further details of the smaller transverse ridges on TR_10 and the extent of flutings are
324 presented in the next section based upon aerial photograph mapping.

325 Ridge complex TR_10 is separated from TR_8, located 130 km to the north, by a wide zone of
326 minor transverse ridges, including the “Lethbridge Moraine” of Stalker (1977), which has been
327 developed on the northern slopes of Milk River Ridge and in the Milk River drainage basin.
328 Immediately south of the Lethbridge Moraine lies a 45 km wide and 150 km long arc of low
329 amplitude, minor transverse ridges (TR_9; Fig. 2b), associated with numerous ridge-parallel
330 meltwater channels and coulees (Fig. 8E). This landform assemblage has been mapped at
331 greater detail using aerial photographs and is reviewed in the next section as a landsystem
332 indicative of lobate terrestrial ice stream margins.

333 Two further sets of minor transverse ridges (TR_11 & TR_12) are located at the south west
334 corner of Ó Cofaigh et als. (2010) ‘Ice Stream 1’. These landforms record the incursion of the
335 “east lobe” onto the northern slopes of the Cypress Hills and against the east side of the Suffield
336 Moraine (Fig. 2).

337 Hummocky terrain covers a large proportion of the study area and defines the margins of
338 palaeo-ice stream/lobe tracks (cf. Evans 2000; Evans et al. 2008). It occurs primarily between
339 the smoothed fast ice flow corridors (Fig. 8B) but also along the southern margin of the CAIS
340 (Figs. 2 & 9). The SRTM and Landsat ETM+ imagery reveals a pattern of hummocky terrain
341 that is similar to that depicted by Prest et al. (1968), Shetsen (1987, 1990), Clark et al. (1996)
342 and Evans (2000). Detailed mapping of the landforms that occur in the hummocky terrain belts,
343 particularly in the McGregor Moraine (Fig. 9), has previously revealed that they comprise areas
344 of linear to chaotic hummock chains interspersed with minor ridges, interpreted by Evans (2000,
345 2009) and Evans et al. (2006) as a landform imprint of glacier margins that alternated between
346 polythermal and temperate in nature during recession. Significantly in this respect, hummocky
347 terrain bands (Stalker's 1977 "Lethbridge Moraine") run continuously from the edge of
348 Blackspring Ridge across the CAIS marginal area up to and around the Cypress Hills. In plan
349 form the bands demonstrate a strong lobate pattern and run parallel to intervening belts of
350 transverse ridges, even though they internally consist of chaotic hummocks. The SRTM data
351 reveal that the hummocky terrain and associated minor ridges are superimposed on larger
352 physiographic features (Fig. 9a), which are likely representative of remnant uplands in the
353 preglacial land surface (Fig. 1c; cf. Leckie 2006). The details of the hummocky terrain and
354 associated minor ridges are presented at larger scale in the next section through a case study of
355 the CAIS ice-marginal landsystem.

356

357 Eskers are prominent on the small scale imagery throughout the study area as narrow winding
358 ridges, but resolution constraints allowed the identification of only the largest features. Future
359 research will concentrate on the mapping of eskers at a much higher resolution using aerial
360 photography and ground survey. The largest esker identified in this study was 45 km long and
361 situated along Hfs_4 (Fig. 10). Further south, a sequence of prominent eskers is situated along
362 the centre of the HPIS corridor, particularly in association with Hfs_5 (Figs. 2 & 4), forming a
363 40 km long network running parallel to lineation direction. Another prominent network of
364 eskers is located along the eastern edge of Lake Newell and emerges 20 km south of CAfs_1
365 and terminates just south of Lake Newell at the inflexion point of the dual-lobate ridge TR_8

366 (see above; Fig. 5; cf. Evans 1996, 2000). Additional eskers were identified along the centre and
367 eastern half of the CAIS.

368

369 **4.2 Ice stream/lobe marginal landsystem: large scale mapping case study of the CAIS**

370 Although ice flow transverse ridges have been identified at a regional scale, as described above
371 (Figs. 2, 4-8), landform mapping from aerial photographs in combination with the SRTM data
372 (Fig. 11) reveals a complex glacial geomorphology at larger and more localized scales,
373 comprising minor transverse ridges, hummocky terrain, flutings and meltwater
374 channels/spillways. These features have been developed on a land surface characterized by
375 Tertiary gravel-capped monadnocks (e.g. Del Bonita uplands/Milk River Ridge, Cypress Hills)
376 and substantial depressions related to long term drainage networks (e.g. Pakowki Lake
377 depression). Previous research has investigated the nature and origins of minor transverse ridges
378 at the margins of the HPIS and CAIS in the McGregor Moraine belt, concluding that spatial
379 variability in morphology (controlled moraine to push moraine) likely reflects changes in the
380 basal thermal regime of the ice sheet margin during recession (Evans et al. 2006; Evans 2009).
381 In order to test this hypothesis, the minor transverse ridge assemblages that demarcate the
382 receding lobate margins of the CAIS are now analysed in detail.

383 Transverse ridges are aligned obliquely to former ice flow and are in places contiguous with
384 bands of hummocky terrain, forming large arcuate bands and thereby allowing the regional
385 lobate pattern of ice stream marginal deposition to be mapped (see above). At larger scales the
386 transverse ridges display significant variability in form and thereby inform a higher resolution
387 palaeoglaciology. The majority of transverse ridges are located to the south and south-east of
388 the Lethbridge Moraine and Etzikom Coulee and the most extensive sequences lie directly south
389 of Crow Indian Lake, Verdigris Coulee and south east of Pakowki Lake (Fig. 11), where they
390 document the early recessional phases of the CAIS margin. Within the CAIS marginal setting
391 three types of minor transverse ridge sets are identified and classified as MTR Types 1-3 (Figs.
392 12-15). Additionally, three types of hummocky terrain form are recognized and classified as
393 Types 1-3 (Figs. 16 & 17).

394

395 MTR Type 1 have largely symmetrical cross profiles and consistent wavelengths (Fig. 12),
396 occur only in the south east corner of the CAIS margin on the TR_10 ridge complex (Figs. 2, 7
397 & 11) and are large enough to be identified in the regional mapping using the SRTM data (Fig.
398 7). Because of its ripple-like appearance in plan form, the TR_10 ridge complex has been
399 interpreted by Beaney and Shaw (2000) as an erosional surface scoured by subglacial
400 megaflood waters. Our large scale mapping reveals that the complex ridge TR_10 comprises
401 three sub-sets of component ridges (Fig. 13). Ridge Set 1A comprises large sub-parallel ridges
402 lying up ice and perpendicular to CAfs_2, and characterised by long wavelengths and
403 intervening hollows filled with numerous small lakes (Fig. 11 & 13). Aerial photographs also
404 reveal that the ridges are more widely overprinted by flutings than was apparent from the SRTM
405 image (Fig. 7). Ridge Set 1B lies parallel to Set 1A but is located adjacent to the more
406 prominent flutings that comprise flow set CAfs_2 and appears as very subtle, discontinuous and
407 densely spaced ridges that have some resemblance to MTR Type 2 (see below). The ridges
408 reach up to 1 km long and are no greater than 2 m high. Ridge Set 1C is located down ice of Set
409 1A and just north of Set 1B (Figs. 11 & 13) and individual ridges are 1-3 km long and resemble
410 the smaller ridges within Set 1A, with similar smooth crests and water filled depressions. They
411 are conspicuous by their north-south orientation, which is approximately 45° offset from the
412 CAfs_2 lineament direction.

413

414 MTR Type 2 are characterized by low relief and sharp crested ridges with largely asymmetrical
415 cross profiles and variable wavelengths; ridges often locally overlap or overprint each other and
416 possess crenulate or sawtooth plan forms (Fig. 12; Evans 2003). They lie primarily on the flat
417 terrain between Pakowki Lake and the MTR Type 1 ridges (Fig. 8D), south of Milk River (Fig.
418 11 & 13) and are characterised by conspicuous ridge sets up to 5 m in high and with generally
419 continuous crests (Fig. 14). The ridges located along the south east margin of Pakowki Lake
420 extend for up to 15 km, but in general the ridges range from 1-5 km long. The ridges situated
421 south of the Milk River (Fig. 11) are more subtle and smaller than those to the south east of

422 Pakowki Lake. In addition to this extensive area of MTR Type 2 ridges, isolated examples of
423 the type occur throughout the study area.

424

425 MTR Type 3 are characterized by discontinuous, low relief and sharp crested ridges that are
426 aligned parallel and contiguous with chains of hummocks to form continuous lines when viewed
427 over large areas. Between the high points, strongly orientated depressions, often filled with
428 ponds and occasionally containing isolated hummocks, accentuate the overall linearity (Figs. 12
429 & 15). They are the most common ridge type located to the west of Pakowki Lake, and are most
430 extensive just south of Etzikom Coulee and Verdigris Coulee (Fig. 11). Individual ridges and
431 associated hummocks are more subtle than MTR Type 2, with smoothed crests and heights
432 generally no greater than 3 m. They also show clear lobate form on both the regional and large
433 scale geomorphology maps (Fig. 2 & 11), and are located on the inclined slope of the CAIS
434 marginal area (Fig. 8A). Like MTR Type 2, the Type 3 ridges also demonstrate subtle
435 overlapping or overprinting (Fig. 15a).

436

437 Hummocky terrain is the most common landform within the CAIS marginal zone, and contains
438 a wide range of hummock types (Figs. 16-18). At large scales, hummock assemblages are
439 chaotic and demonstrate little to no linearity but when viewed at smaller scales they exhibit
440 curvilinear or lobate patterns aligned parallel to sequences of transverse ridges (Figs. 2 & 11).
441 North of Etzikom Coulee several long thin hummocky terrain bands run parallel to transverse
442 ridges and meltwater channels. The largest extends for 60 km from west of 112°0'0"W,
443 between Etzikom and Chin Coulee eastwards to the north of Pakowki Lake (Fig. 11). This
444 hummocky terrain forms part of the "Lethbridge Moraine" which extends from Lethbridge to
445 the north slopes of the Cypress Hills (Fig. 2; Westgate, 1968; Bik, 1969; Stalker 1977).
446 Hummocky terrain also occurs in the south west corner of the study area, where it wraps around
447 the Del Bonita Highlands and along the Milk River Ridge. Close inspection of these hummocky
448 terrain bands reveals three different types of hummock (Types 1-3; Fig. 17).

449 Type 1 hummocks form the majority of the hummocky terrain and consist of densely spaced,
450 low relief hummocks with little or no orientation (Figs. 16 & 18). The hummocks vary
451 significantly in size, up to 5 m in height and generally <30 m in diameter (Fig. 17). Their
452 morphology varies from individual circular and oval shaped hummocks to interconnected larger
453 hummocks with less rounded tops. Type 1 and Type 2 hummocks lie randomly juxtaposed with
454 each other and make up 99% of the hummocky terrain bands. Numerous small ponds fill the
455 depressions between the hummocks.

456 Type 2 hummocks are generally randomly juxtaposed with Type 1 but also form occasional
457 larger zones within other hummocky terrain bands (Fig. 16c). They are characterised by circular
458 mounds with a cylindrical, often water filled, hollow at their centre (Fig. 17). This creates a ring
459 or “doughnut” shape that is noticeably different in morphology to Type 1 hummocks.
460 Conspicuous ridges also occur within the larger zones of Type 2 hummocks (Fig. 18a). These
461 ridges weave through the hummocks, showing no singular orientation, and occasionally make
462 up parts of the rims of hummocks.

463 Type 3 hummocks are the largest of the hummock types, being up to 20 m high and 1 km wide
464 (Fig. 17). They have a roughly cylindrical to oval plan form and are up to twice as high as the
465 surrounding hummocky terrain. Some have large rims and all have a flat surface. They are the
466 least common of the three hummock types but the most conspicuous. Type 3 hummocks are
467 best developed and primarily located in the south west corner of the study area around the Del
468 Bonita Highlands (Fig. 18a).

469

470 Flutings near the margin of the CAIS are located predominantly along the eastern portion of the
471 Milk River and south and south east of Pakowki Lake, but also north of Tyrrell Lake (Fig. 11).
472 They range from 1-9 km in length with an average of 2 km. Flutings located north and south of
473 the Milk River clearly overprint MTR Type 1 (Figs. 11 & 13) at right angles and are less than 2
474 m in amplitude, making them difficult to recognise on the ground (Westgate, 1968). The
475 flutings that constitute flow set CAfs_2 are notably larger than any other lineations in the CAIS
476 marginal zone, individuals being up to 9 km long and 6 m high and the whole flow set covering

477 an area 30 km long and 5 km wide. As a result the areal photographs reveal at least double the
478 amount of flutings compared to the SRTM data. This scale of resolution allows further
479 assessment of fluting dimensions, including elongation ratios, which range from 12:1 up to 85:1
480 along the CAfs_2 with fluting length increasing in a down flow direction.

481

482 Four major spillways extend across the study area, including Forty Mile Coulée, Chin Coulée,
483 Etzikom Coulée and Verdigris Coulée, and lie parallel to the transverse ridges, conforming to
484 the lobate plan form displayed by the ice-marginal landform record (Fig. 11). They extend
485 across the majority of the “Lethbridge Moraine” sequence as dominant features, reaching up to
486 500 m wide and 60 m deep (Fig. 19). An extensive network of smaller channels situated north
487 of Chin Coulée (Fig. 11 & 19) lie predominantly parallel but also perpendicular to the spillway.
488 These shallow channels are up to 10 km long and 200 m wide (Fig. 19). Longer channels up to
489 20 km long and 100 m wide are found to the north of Crow Indian Lake, dissecting the
490 hummocky terrain band at right angles. Only a few eskers were identified and are located
491 chiefly in the north east corner of the area mapped in Figure 11.

492

493 **5. Interpretations of geomorphology mapping**

494 **5.1 Smoothed corridors, lineations and flutings**

495 Smoothed “corridors” of terrain on the plains of western Canada have been previously
496 interpreted as palaeo-ice stream tracks or footprints (Evans et al. 2008; Ó Cofaigh et al. 2010)
497 based upon the geomorphological criteria proposed by Stokes and Clark (1999, 2001; Table 2).
498 The “corridors” contain MSGL or flutings and are delineated by a change in smoothed
499 topography, created by fast ice flow, to hummocky terrain associated with slow moving, cold
500 based ice and stagnation (Dyke & Morris 1988, Stokes & Clark 2002, Evans et al. 2008; Evans
501 2009; Ó Cofaigh et al. 2010). Similarly, we here compare the lineations and smoothed
502 topography of southern Alberta to previously identified palaeo-ice streams (Patterson 1997,
503 1998; Stokes and Clark, 1999, 2001; Clark and Stokes, 2003; Jennings, 2006) and to the
504 forelands of contemporary ice streams on the Antarctic Shelf (Shipp et al., 1999; Canals et al.,
505 2000; Wellner et al., 2001; Ó Cofaigh et al., 2002), and thereby substantiate proposals for the

506 former occurrence of the HPIS and CAIS in the southwest Laurentide Ice Sheet. The onset
507 zones of both the HPIS and CAIS are unknown and mapping by Prest et al. (1968) and Evans et
508 al. (2008) do not identify any clear convergent flow patterns. However, till pebble lithology data
509 (Shetsen 1984) demonstrate a Boothia type (Dyke & Morris 1988) dispersal by the HPIS and
510 CAIS. Based on the reconstructed flow sets and landforms it seems clear that both the HPIS and
511 CAIS represent ‘time-transgressive’ ice streams (Clark and Stokes, 2003).

512

513 Topographic cross profiles (Fig. 8B) and topographic maps (Geiger 1967) reveal that the CAIS
514 is a ‘pure’ ice stream and the HPIS a predominantly ‘topographic’ Ice stream (Clark and Stokes,
515 2003). The HPIS traversed across the easterly sloping terrain of the High Plains (Hfs_2-5; Fig.
516 3), but Cordilleran and Laurentide ice coalescence during the LGM forced the HPIS to flow in a
517 southeasterly direction, as highlighted by the different orientations of Hfs_1 and Hfs_2-5 (Fig.
518 3). Additionally, the 90° shift of the HPIS between Hfs_1 and 2 (Fig. 3) is positioned
519 approximately where the Foothills Erratics train is located, which has been used to mark the
520 location of ice sheet coalescence (Stalker, 1956; Jackson et al., 1997; Rains et al., 1999). The
521 multiple flow-sets along the HPIS therefore document numerous small scale flow re-
522 organisations during deglaciation controlled by lobation of the ice stream margin. Hfs_5 (Fig.
523 3) is composed of numerous lineations that on a small scale demonstrate strong spatial
524 coherency. However, large scale mapping compiled by Evans et al. (2006) identifies cross
525 cutting lineations which must have been formed during more than one flow event.

526

527 Few flow sets were identified along the CAIS track and a lack of obvious cross-cutting patterns
528 hampers any identification of changing flow directions. However, the orientation of flow set
529 CAfs_1 appears to relate to lobate ice flow towards the dual lobate ridge TR_8 (Figs. 3 & 5),
530 indicating that TR_8 could represent the maximum position of a re-advance during which flow
531 set CAfs_1 was aligned obliquely with the lobate ice margin. Transverse ridge sets TR_6 and
532 TR_7 appear to represent later readvances by the CAIS lobe that terminated north of TR_8. This
533 would explain the streamlining of a major esker network by CAfs_1 to the north of TR_6 and
534 TR_7 and its preservation in a non-streamlined state to the south (Evans 1996, 2000), where it

535 documents the development of a significant subglacial/englacial drainage pathway at the
536 junction of two ice flow units in the CAIS; the latter is indicated by the dual lobate TR_8 ridge
537 and the coincidence of the esker complex at the apex of the ridge re-entrant (Fig. 5; see *Section*
538 *ii* below).

539

540 In the marginal zone of the CAIS in south and south east Alberta (Fig. 11), MSGL and smaller
541 flutings overprint MTR Types 1 and 2, specifically to the south and south east of Lake Pakowki.
542 Because the streamlining of the MTR is mostly only cosmetic, their construction and overriding
543 was likely not related to initial advance of the ice sheet to its LGM limit but rather a localized
544 re-advance of the ice sheet margin; potential candidates are the Altawan advance of Kulig
545 (1996) and the Wild Horse advance of Westgate (1968). This advance impacted on the terrain
546 between the Cypress Hills and the longitude of 112°W, approximately 15 km east of Del Bonita.
547 The minor flutings in the area run parallel to flow set CAfs_2 and so, based on their strong
548 parallel coherency, are interpreted to represent the same flow event. Lineation length gradually
549 increases from northwest to southeast, trending into several MSGLs within CAfs_2 (Fig. 11).
550 All measured ERs within the CAIS marginal area are greater than the 10:1 minimum threshold
551 proposed by Stokes and Clark (2002) for fast flowing ice.

552

553 The locations of CAfs_1 and 2 (Fig. 3) on the down ice side of bedrock highs that appear to
554 have been glacitectonically thrust and stacked (see *Section iii* below) and at locations where the
555 proglacial slope dips down ice (Fig. 8A & D), suggest that topography may have been a
556 controlling factor in their production. Similar lineation occurrences on the down ice sides of
557 higher topography are found within Hfs_5 on Blackspring Ridge (Fig. 2; Munro-Stasiuk &
558 Shaw 2002) and the Athabasca fluting field in central Alberta (Shaw et al., 2000), an
559 observation also made by Westgate (1968), who further highlights the occurrence of the largest
560 flutings in such settings. If this is a significant factor in lineation and MSGL production, it
561 would explain why there are so few lineations along the CAIS where the regional slope
562 predominantly dips up ice (Fig. 8A). This evidence is consistent with the groove ploughing
563 theory for lineation production (Clark et al., 2003) whereby ice keels produced by flow over

564 bedrock bumps carve grooves in the bed and deform sediments into intervening ridges or
565 flutings. The surface form of the northern end of the megafluting complex at the centre of
566 CAfs_1 is instructive in this respect in that it appears as a flat-topped ridge with grooves in its
567 summit (Evans 1996, 2000).

568

569 **5.2 Transverse ridges**

570 A variety of large transverse ridges were initially identified on DEMs by Evans et al. (2008)
571 who interpreted them as either overridden or readvance moraines based upon their morphology
572 and some localized exposures, the latter indicating a glacitectonized bedrock origin. The higher
573 resolution SRTM data used in this study facilitate a more detailed assessment of these forms.

574

575 The streamlining and lineation overprinting of the two major arcuate ridges within the TR_1
576 sequence (Figs. 2 & 4) document the southerly advance of the HPIS over the site after major
577 ridge construction. The arcuate nature of the ridges indicates that they were constructed as ice
578 marginal features and so likely record an earlier advance of the HPIS to this location. The two
579 major ridges occur at a location where the bedrock topography rises 30-60 m above the
580 surrounding terrain (Geiger, 1967) and are significantly different in morphology to the minor
581 ridges that lie over, between and south of them (Fig. 2). Their size, multiple crests and location
582 on a bedrock rise are compatible with glacitectonic origins, similar to numerous other examples
583 in southern Alberta, where the Cretaceous bedrock is highly susceptible to disruption due to
584 glacier advance (Bluemle & Clayton 1984; Aber et al., 1989; Aber & Ber 2007).

585

586 Similarly, in the east, ridge sets TR_3 & 4 (Fig. 2) are locally known as the Neutral Hills and
587 have been traditionally recognized as glacitectonic thrust block moraines (Moran et al. 1980;
588 Aber & Ber 2007). Previous mapping in the area of TR_3 by Kjearsgaard (1976) and Shetsen
589 (1987) identified significantly fewer transverse ridges but did propose an ice thrust origin. Ice
590 thrusting was also proposed by Kjearsgaard (1976), Shetsen (1987) and Evans et al. (2008) for
591 ridge set TR_4. Glacitectonic origins are also most likely for TR_5 & 6 (Fig. 2), because they
592 occur on bedrock highs (Fig. 8A) and hence are influenced by topographical controls (Tsui et al.

593 1989; Bluemle & Clayton 1984; Aber et al., 1989), comprise closely spaced, parallel and
594 predominantly linear multiple ridge crests, and internally contain glactectonized bedrock
595 (Evans & Campbell 1992; Evans 1996; Evans et al. 2008). The overall arcuate plan forms of
596 both TR_5 and TR_6 also supports an ice-marginal origin. Based on this evidence both sets of
597 ridges are interpreted as ice thrust ridges formed by compressive ice marginal flow (cf. Evans,
598 1996, 2000; Evans et al., 2008). A thin till cover situated on top of the ridges suggests that they
599 are actually cupola hills (Aber et al. 1989; Benn & Evans 2010; Evans 2000) produced by the
600 overriding CAIS margin (Evans, 2000). Ridge set TR_7 is a locally fluviially modified part of
601 sequence TR_6 and so it is most likely that they share similar origins.

602

603 The large dual-lobate ridge (TR_8) has previously not been identified and is hereafter named the
604 “Vauxhall Ridge” after the nearest town. It is almost certainly ice marginal, based on its dual-
605 lobate plan form, and lies down ice and perpendicular to CAfs_1 and the subglacially
606 streamlined Lake Newell esker complex (Fig. 5; Evans 1996), which suggests that it records the
607 re-advance limit of the CAIS. The ridge also continues into hummocky terrain and transverse
608 ridges to the east, which are therefore interpreted to have formed contemporaneously. The
609 geomorphic expression of the Vauxhall Ridge provides few indicators as to its precise genetic
610 origins, and so further investigation of sub-surface structure is required.

611

612 Ridge sets TR_11 & 12 (Fig. 2) are interpreted as a single sequence of ridges formed at the
613 margin of the “east lobe” or ‘Ice Stream 1’ of Ó Cofaigh et al. (2010). Extensive sections
614 through the ridges show that they have been glactectonically thrust and stacked (Ó Cofaigh et
615 al. 2010), indicating an ice thrust origin.

616

617 Similar glactectonic origins are proposed for some of the transverse ridges mapped at larger
618 scales in the CAIS margin case study. Specifically, all three sub-types of the MTR Type 1
619 ridges of the CAIS marginal landsystem (TR_10; Fig. 2) likely originated through glactectonic
620 thrusting and have been overrun by a re-advancing ice margin. The largest ridges (Set A, Fig.
621 13) are overprinted with lineations and their tops have been smoothed by ice flow. The ridges

622 are composed of deformed bedrock (Beaney & Shaw 2000), an observation used to support a
623 proglacial thrusting origin by Westgate (1968), Shetsen (1987) and Evans et al. (2008). Their
624 location along the preglacial drainage divide suggests that topography was significant in their
625 formation; glacier flow would have been compressive (Fig. 8D) and porewater pressures in the
626 weak Cretaceous bedrock would have been elevated, a situation highly conducive to
627 glacitectonism (Bluemle & Clayton 1984; Aber et al. 1989; Tsui et al. 1989). Although a
628 glacitectonic origin is the most appropriate interpretation for ridge Type 1A, MTR Types 1B
629 and 1C display more subtle characteristics that hamper confident process-form interpretations.
630 Type 1B ridges (Fig. 13) have been heavily modified by glacier re-advance and are barely
631 distinguishable in the landform record. Their orientation parallel to Type 1A ridges suggests
632 that they formed during the same advance and therefore possibly by the same mechanism,
633 although initial relief was modest. Type 1C ridges are very similar in form to Type 1A ridges
634 but have been significantly modified into more subtle and smoothed features. Based on their
635 similar morphology and location on the preglacial divide they are also interpreted as overridden
636 thrust ridges.

637

638 MTR Type 2 sequences (Fig. 12), primarily located east and south east of Pakowki Lake and
639 south of the Milk River (Figs. 8D, E & 11), display an inset (en echelon) pattern that closely
640 resembles that of push moraines presently developing at active temperate glaciers, for example
641 at Breiðamerkurjökull and Fjallsjökull in Iceland (Price 1970; Sharp 1984; Boulton 1986;
642 Matthews et al. 1995; Krüger 1996; Evans & Twigg 2002; Evans 2003; Evans & Hiemstra
643 2005). These modern analogues have been used by Evans et al. (1999, 2008) and Evans (2003)
644 to support the interpretation of the whole sequence of transverse ridges within the CAIS
645 marginal area as recessional push moraines, a more specific genetic assessment than the
646 previous conclusions of Westgate (1968) that the landforms represented “washboard moraine”,
647 “linear disintegration ridges” and “ridged end moraine”. A recessional push moraine origin
648 implies that the CAIS margin must have been warm based during landform construction,
649 reflecting seasonal climate variability (Boulton 1986; Evans & Twigg 2002; Evans 2003).

650

651 The origins of MTR Type 3 are indicated by the style of hummock (see section *iv* below) visible
652 within the linear assemblages that make up the component ridges. The individual hummocks
653 that predominate within MTR Type 3 vary between Type 1 and Type 2 hummocks, which are
654 interpreted below as having formed supraglacially. This implies that significant englacial debris
655 concentrations characterized the margin of the CAIS at the time of MTR Type 3 formation.
656 Debris provision could have been related to either englacial thrusting and stacking of debris rich
657 ice due to compressive flow against the reverse regional slope (Fig. 8A; Boulton, 1967, 1970;
658 Ham & Attig, 1996; Hambrey et al., 1997, 1999; Glasser & Hambrey, 2003) or incremental
659 stagnation (Eyles, 1979; 1983; Ham & Attig, 1996, Patterson, 1997; Jennings, 2006; Clayton et
660 al., 2008; Bennett & Evans 2012). In the case of incremental stagnation, the moraine linearity
661 would be related to either the high preservation potential of controlled moraine (Gravenor &
662 Kupsch, 1959; Johnson & Clayton, 2003), an unlikely scenario based upon modern analogues of
663 controlled moraine development (Evans, 2009; Roberts et al., 2009), or active recession of a
664 debris charged ice margin brought about by warm polythermal conditions and accentuated by
665 upslope advances (Evans 2009). This is supported by the fact that, although MTR Type 3
666 sequences are composed of contiguous linear hummock tracks and discontinuous ridges (Figs.
667 11, 12, 14 & 15), small scale mapping (Fig. 2) shows clear inset sequences of MTR Types 2 and
668 3, typical of active recession of both the CAIS and HPIS margins in southern Alberta (note that
669 the minor ridges in TR_1 are MTR Types 2 & 3) based upon modern analogues of active
670 temperate and warm polythermal glaciers (Boulton 1986; Evans & Twigg 2002; Colgan et al.
671 2003; Evans 2003, 2009; Evans & Hiemstra 2005).

672

673 **5.3 Hummocky terrain**

674 Type 1 hummocks represent the largest proportion of hummocky terrain within the CAIS
675 marginal area. Concentrations of Type 1 hummocks occur around the Del Bonita highlands and
676 in the lobate bands of hummocks north of Etzikom Coluée (Fig. 11), also known as the
677 Lethbridge moraine (Stalker, 1977). Previous work in Alberta (Gravenor & Kupsch, 1959;
678 Stalker, 1960; Bik, 1969) has identified that a significant proportion of Type 1 hummocks are
679 composed of till. A supraglacial origin for Type 1 hummocks can be supported by simple form

680 analogy (cf. Clayton, 1967; Boulton, 1967, 1972; Parizek, 1969; Clayton & Moran, 1974; Eyles,
681 1979, 1983; Paul, 1983; Clayton et al., 1985; Johnson et al., 1995; Ham & Attig, 1996;
682 Patterson, 1997, 1998; Mollard, 2000; Johnson & Clayton, 2003; Jennings, 2006), but their
683 juxtaposition with active recessional moraines in lobate arcs of landform assemblages (Fig. 11
684 & 16) suggests that they were not associated with widespread ice stagnation. Differential
685 melting and supraglacial debris reworking by continuous topographic reversal can be invoked to
686 explain the irregular shapes and sizes of the hummocks when viewed at larger scales, although
687 subglacial pressing of the soft substrate at the margin of the CAIS, as proposed by Stalker
688 (1960), Eyles et al. (1999) and Boone and Eyles (2001), could have been operating in the poorly
689 drained conditions of the reversed proglacial slopes of the region (Klassen, 1989; Mollard
690 2000). Nevertheless, the lobate arcuate appearance of Type 1 hummocks when viewed at
691 smaller scales has a strong resemblance to the controlled moraine reported by Evans (2009) and
692 the hummock assemblages along the southern Laurentide Ice Sheet margins described by
693 Colgan et al. (2003) and Johnson and Clayton (2003) as their “Landsystem B”. The corollary is
694 that, during early deglaciation, the edge of the CAIS was cold based and part of a polythermal
695 ice sheet margin, beyond which there was a permafrost environment (Clayton et al. 2001;
696 Bauder et al. 2005); several generations of ice wedge casts around the Del Bonita (Jan
697 Bednarski, personal communication) and the Cypress Hills uplands (Westgate, 1968) verify
698 ground ice development around the receding CAIS margin.

699

700 North of the CAIS marginal zone, Type 1 hummocks are extensive and well developed, and
701 therefore have been the subject of numerous investigations (e.g. Stalker, 1960, Munro-Stasiuk
702 and Shaw, 1997; Eyles et al., 1999; Boone and Eyles, 2001; Evans et al., 2006). Comparison of
703 Figure 2 and existing maps (cf. Shetsen, 1984, 1987; Clark et al., 1996; Evans et al., 1999)
704 shows that hummocky terrain mapping using SRTM data is capable of a high degree of
705 replication. Due to its position between corridors of fast flowing ice lobes, the hummocks have
706 been used to demarcate an ‘interlobate’ terrain by Evans et al. (2008), but the more generic term
707 ‘hummocky terrain’ is preferred here. Nonetheless, the abrupt transition from smoothed
708 topography (corridor) to hummocky terrain along the CAIS margin is interpreted as a change in

709 subglacial regime, and hence demarcates the flow path of the ice stream (cf. Dyke & Morris
710 1988; Patterson 1998; Evans et al. 2008; Ó Cofaigh et al. 2010). Glacitectonic evidence
711 identified along the north shore of Travers Reservoir, demonstrates that some linear hummocks
712 and low amplitude ridges in hummocky terrain are in fact thrust block moraines (Evans et al.,
713 2006) formed by ice flow from the north east, indicative of CAIS advance into the area after the
714 HPIS had receded. The input from the HPIS is demarcated by flow sets Hfs_4 and 5 (Fig. 3)
715 which flow into the ‘McGregor moraine’. Detailed investigation of this area by Evans et al.
716 (2006) reveals that the hummocky terrain, when viewed at large scale, comprises inset
717 recessional push ridges and associated arcuate zones of flutings similar to modern active
718 temperate glacial landsystems (Evans et al. 1999; Evans & Twigg, 2002; Evans 2003; Evans et
719 al. 2006; Evans et al. 2008). The hummocky terrain therefore represents a less linear set of ice-
720 marginal landforms to those with which it is laterally continuous in the HPIS trunk immediately
721 to the west (Fig. 2). The reconstructed ice margins show that ice was flowing into the area from
722 the northwest (Evans et al., 2006), and so most likely represent the termination of flow set
723 Hfs_5.

724

725 Type 2 hummocks resemble the “doughnut hummocks” or “ring forms” that are common to
726 many deglaciated ice sheet forelands in mid-latitude North America and Europe (e.g. Gravenor
727 & Kupsch 1959; Parizek 1969; Aartolahti 1974; Lagerbäck 1988; Boulton & Caban 1995;
728 Mollard 2000; Colgan et al. 2003; Knudsen et al. 2006). Johnson and Clayton (2003)
729 demonstrate that doughnut hummocks across North America are predominantly composed of
730 clayey till, which they suggest is important to hummock formation. Several genetic models have
731 been proposed, all of which regard the landforms as indicative of a ‘stagnant glacial regime’
732 (Knudsen et al. 2006), but they remain poorly understood. Importantly, like Type 1 hummocks,
733 the fact that Type 2 hummocks are often contiguous with push ridges appears to contradict the
734 stagnation model. Because Type 2 hummocks are contiguous with not only recessional push
735 moraines but also Type 1 and Type 3 hummocks (see below), which are supraglacial in origin,
736 it follows that doughnut hummocks most likely also originated as supraglacial debris
737 concentrations (controlled moraine) in a polythermal ice sheet margin. Alternative origins for

738 Type 2 hummocks include proglacial blow-out features created by over-pressurized
739 groundwater (Bluemle 1993; Boulton & Caban 1995; Evans et al 1999; Evans 2003, 2009) and
740 subglacial pressing of saturated sediments (Gravenor & Kupsch 1959; Stalker 1960; Aartolahti
741 1974; Eyles et al. 1999; Mollard 2000; Boone & Eyles 2001), although the latter would not
742 produce linear chains of hummocks lying between arcuate push moraine ridges.

743

744 The conspicuous ridges that occur in association with Type 2 hummocks (Fig. 18a) and are
745 often continuous with hummock rims must document the more extensive operation of the rim
746 forming process. This could involve either: a) the elongation of hollows between controlled
747 moraines during melt-out, giving rise to preferential deposition in linear chains of ice-walled
748 channels or supraglacial trough fills (Thomas et al. 1985); and/or b) occasional ice-marginal
749 pushing during the overall downwasting of a debris-charged snout upon which controlled
750 moraine was developing (cf. Evans 2009; Bennett et al. 2010; Bennett & Evans 2012).

751 Type 3 hummocks closely resemble the ice-walled lake plains of the southern Laurentide lobes
752 in Minnesota, North Dakota, Wisconsin, Michigan and southern New England (Colgan et al.,
753 2003; Clayton et al., 2008) and throughout Europe (Strehl, 1998; Knudsen et al., 2006). Strong
754 evidence presented by Clayton et al. (2008) demonstrates that ice-walled lake plains cannot be
755 of subglacial origin based on molluscs present within the enclosed deposits. Their presence
756 therefore is unequivocally associated with supraglacial origins, the corollary of which is that
757 any adjacent hummocky terrain is also of supraglacial origin (Johnson & Clayton 2003; Clayton
758 et al., 2008). The large sizes of the Type 3 hummocks can be explained by their continued
759 development after ice recession due to a thick insulating debris cover (Attig, 1993; Clayton et
760 al., 2001; Attig et al., 2003; Clayton et al., 2008), hence also their absence from the active
761 recessional imprint of the CAIS marginal area. The close association between ice-walled lake
762 plain development and permafrost (Attig, 1993; Clayton et al., 2001; Attig et al., 2003) is also
763 evident within the CAIS marginal area, whereby the largest ice-walled lake plains are located
764 around the Del Bonita Highlands where permafrost features have also been recorded
765 (Bednarski, personal communication).

766

767 **6. Discussion**

768 **6.1 Overview and chronology**

769 The regional glacial geomorphology of southern Alberta primarily records the deglacial
770 dynamics of the south west margin of the Laurentide Ice Sheet, within which three major ice
771 streams (HPIS, CAIS of Evans et al. 2008 and “Ice Stream 1” or “east lobe” of Ó Cofaigh et al.
772 2010 and Shetsen 1984 respectively) coalesced and flowed against the north-easterly dipping
773 topography, thereby damming proglacial lakes and diverting regional drainage during advance
774 and retreat (Shetsen 1984; Evans 2000; Evans et al. 2008). In combination with the available
775 deglacial chronology for the region (cf. Westgate 1968; Clayton & Moran 1982; Dyke & Prest
776 1987; Kulig 1996) the ice-marginal landforms are now used to chart ice sheet retreat patterns
777 (Fig. 20).

778

779 Although the existing chronology is not well constrained by absolute dates, it is appropriate to
780 acknowledge Westgate’s (1968) five distinct morphostratigraphic units (Elkwater drift; Wild
781 Horse drift; Pakowki drift; Etzikom drift; Oldman drift), each of which has been taken to
782 represent a re-advance limit in south east Alberta based on petrography and morphology. The
783 Elkwater drift relates to the upper ice limit on the Cypress Hills. The Wild Horse drift extends
784 into northern Montana where it terminates at a large 15-20 m transverse ridge sequence and is
785 interpreted to represent the final advance of the CAIS margin into Montana sometime around 14
786 ka BP. The Pakowki drift (Fig. 20) is marked by the outer extent of the push moraines to the
787 south east of Lake Pakowki and runs along the northern tip of the Milk River and north around
788 the Cypress Hills (Wesgate, 1968; Bik, 1969; Kulig, 1996). Therefore, all landforms to the
789 south of this point were formed during an earlier advance, most likely the Altawan advance
790 (15ka BP; Kulig, 1996). The Pakowki advance (Fig. 20), not recognized in Christiansen’s
791 (1979) or Dyke and Prest’s (1987) deglacial sequences, most likely occurred between 14-13.5
792 ka BP (Kulig, 1996) and relates to Clayton and Moran’s (1982) Stage F - H. The Etzikom drift

793 limit is interpreted as the “Lethbridge moraine” limit of Stalker (1977) and is marked in Figure
794 20 by the broad band of hummocky terrain just north of Etzikom Coulee. This ice margin
795 maintained its position along the Lethbridge moraine until around 12.3ka BP (Stage I, Clayton
796 and Moran, 1982; Dyke and Prest, 1987; Kulig, 1996). The Oldman drift limit (Fig. 20) is
797 located just south of the Oldman River. Importantly, the correlation between the thrust ridges at
798 Travers Reservoir (Evans et al., 2006) and the Oldman limit suggests that they were formed
799 during this re-advance episode. The corollary is that the HPIS had already receded further to the
800 north. This re-advance (Stage J – L, Clayton and Moran, 1982) most likely occurred just after
801 12ka BP. Based on the regional geomorphology map (Fig. 2) it is suggested that a further re-
802 advance occurred (Vauxhall advance), the limit of which is marked by the Vauxhall Ridge and
803 must have occurred sometime after 12ka BP. Evans (2000) suggests that the CAIS margin had
804 receded to the north of the study area by 12ka BP. Based on the Vauxhall advance evidence, the
805 CAIS must have receded later than that proposed by Evans (2000). Importantly, Dyke and Prest
806 (1987) place the ice sheet margin to north of the study area by this time, and so this suggests
807 that the CAIS may have remained within southern Alberta for longer than previously thought.
808 The Vauxhall ridge is interpreted to mark the final re-advance of the CAIS after which time it
809 receded rapidly (Evans, 2000). The exact timing of the HPIS and east lobe retreat are unclear,
810 but it seems likely that the HPIS had receded somewhere north of Bow River by 12ka BP.

811

812 **6.2 Landsystem model of the terrestrial terminating ice stream margin**

813 The juxtaposition of the moraine types of southern Alberta is illustrated in Figure 21a and used
814 in Figure 21b to construct a conceptual landsystem model for terrestrial terminating ice stream
815 margins. This model implies that terrestrial ice stream margins are subject to changing thermal
816 conditions and dynamics, often at small spatial and temporal scales. Various parts of the ice
817 stream beds of western Canada have been interpreted previously as manifestations of specific
818 landsystems based upon similarities with modern analogues; for example, Evans et al. (1999,
819 2008) have identified an active temperate landform signature in the HPIS imprint and a surging
820 signal in the Lac la Biche ice stream. Additionally, switches in basal thermal regime have been
821 invoked by Evans (2009) to explain inset suites of different moraine types associated with the

822 recession of the HPIS margin in the McGregor Moraine belt. Thermal regime switches and
823 intermittent surges during recession have been proposed elsewhere in reconstructions of
824 southern Laurentide Ice Sheet palaeoglaciology. For example, Colgan et al. (2003) identify
825 three characteristic landsystems which they interpret as the imprint of an ice lobe with changing
826 recessional dynamics. The outermost landsystem of a drumlinized zone grading into moderate-
827 to high-relief moraines and ice-walled lake plains represents a polythermal ice sheet margin
828 with sliding and deforming bed processes giving way to a marginal frozen toe zone. Inboard of
829 this landsystem lie fluted till plains and low-relief push moraines, a landsystem indicative of
830 active temperate ice recession. This in turn gives way to a landsystem indicative of surging
831 activity. At a regional scale, Evans et al. (1999, 2008) and Evans (2009) have promoted similar
832 temporal and spatial variability in ice stream landform imprints in Alberta, but the large scale
833 mapping reported here allows a finer resolution record of such changes to be elucidated for ice
834 sheet margins during the early stages of deglaciation.

835

836 **6.3 Dynamics of the Alberta terrestrial terminating ice stream lobes**

837 The Alberta ice streams flowed over a substrate composed of Cretaceous and Tertiary
838 sediments, consisting of poorly consolidated clay, sand and silt. The Cretaceous beds in
839 particular are prone to glacitectonic folding and thrusting due to a high bentonite content, which
840 is reflected by the quantity and size of thrust features within southern Alberta. Additionally, the
841 drainage conditions caused by swelling clays will have almost certainly created elevated
842 porewater pressures and localized impermeable substrates, giving rise in turn to fast glacier flow
843 (Clayton et al., 1985; Fisher et al., 1985; Klassen, 1989; Clark, 1994; Evans et al., 2008).
844 Bedrock highs, many of which are controlled by residual Tertiary gravel caps (monadnocks),
845 will likely have created resistance to ice flow (e.g. Alley, 1993; Joughin et al., 2001; Price et al.,
846 2002; Stokes et al., 2007) and caused localised compression, highlighted by the presence of
847 thrust ridges at such locations. Additionally, the reverse gradient of the easterly dipping bedrock
848 surface will have initiated significant marginal compressive flow which also would have
849 resulted in glacitectonic disturbance and well developed controlled moraine on debris-charged
850 snouts. The region is thereby an ancient exemplar of geologic setting exerting strong controls on

851 the location and flow dynamics of ice streams (Anandakrishnan et al., 1998; Bell et al., 1998;
852 Bamber et al., 2006), although it is difficult to ascertain whether fast ice motion occurred
853 through deformation or sliding or a combination of the two. Numerous till units and up ice
854 thickening till wedges within southern Alberta (Westgate, 1968; Evans & Campbell, 1992;
855 Evans et al., 2008, 2012) are consistent with the theory of subglacial deformation (Alley, 1991;
856 Boulton, 1996a, b), although Evans et al. (2008) argue that the presence of large subglacial
857 channels and thin tills overlying thin stratified sediments and shale bedrock along the CAIS
858 trunk indicates that deformation was subordinate to sliding.

859

860 A clear change in landform assemblages from south to north along the axis of the CAIS
861 documents a temporal change in ice stream/lobe dynamics. Initial advance of the CAIS was
862 responsible for the glacitectonic construction and overriding of large transverse ridges in
863 bedrock (cupola hills). The extent of modification or streamlining of these landforms decreases
864 in a southerly direction, as illustrated by the superficial fluting of TR_10 south of Lake
865 Pakowki, which reflects the short duration of overriding by the CAIS. Long flutings to the south
866 of TR_10 record fast glacier flow or ice streaming when the margin of the CAIS lay in
867 Montana. Although the dynamics of the CAIS during Laurentide Ice Sheet advance are difficult
868 to reconstruct, the construction of large thrust moraines are most commonly associated with
869 surging glacier snouts and therefore this mode of flow during advance cannot be ruled out.
870 During deglaciation the dynamics of the CAIS switched from fast flow/streaming to steady state
871 flow towards a lobate margin with a changing sub-marginal thermal regime. This is recorded by
872 the arcuate bands of MTR Type 1 – 3 ridges and hummocky terrain located between the
873 preglacial divide (Milk River Ridge) and the Bow River catchment. Specifically, the sequential
874 south to north change from hummocky terrain to MTR Type 2 to MTR Type 3 in this area
875 records a temporal switch in ice marginal characteristics, from cold polythermal to temperate
876 and then to warm polythermal (cf. Colgan et al. 2003; Evans 2009). A similar switch in sub-
877 marginal thermal characteristics has been proposed for the HPIS by Benn and Evans (2006) and
878 Evans (2009) to explain a south to north change in moraine characteristics. Based upon the
879 chronology of ice sheet recession presented in Figure 20, it appears that the switch to temperate

880 conditions occurred at approximately the same time in both the CAIS and HPIS, indicating a
881 potential climatic control. A contrasting landform assemblage north of the Bow River basin
882 documents a further change in CAIS dynamics, wherein overridden thrust moraines,
883 megaflutings (CAfs_1) and a fluted esker complex lie inboard of the Vauxhall Ridge. This
884 assemblage is interpreted as the imprint of a fast flow/streaming event, a precursor to the surges
885 that constructed thrust moraines (e.g. TR_3) and crevasse-squeeze ridges to the north of the
886 study area (Evans et al. 1999, 2008). Recession of the CAIS margin is demarcated between the
887 surge limits by inset sequences of marginal and sub-marginal meltwater channels and spillways
888 (Fig. 2).

889

890 **7. Conclusions**

891 Glacial geomorphological mapping from SRTM and Landsat ETM+ imagery and aerial
892 photographs of southern Alberta has facilitated the identification of diagnostic landforms or
893 landform assemblages (landsystems model) indicative of terrestrial-terminating ice stream
894 margins with lobate snouts. Spatial variability in landform type appears to reflect changes in
895 palaeo-ice stream activity and snout basal thermal regimes, which are potentially linked to
896 regional climate controls at the southwest margin of the Laurentide Ice Sheet.

897

898 Small scale mapping case studies of the High Plains (HPIS) and Central Alberta (CAIS) palaeo-
899 ice stream tracks reveal distinct inset sequences of fan-shaped flow sets indicative of receding
900 lobate ice stream margins. The lobate margins are recorded also by large, often glacially
901 overridden transverse moraine ridges, commonly constructed through the glacitectonic thrusting
902 of bedrock, and smaller, closely spaced inset sequences of recessional push moraines and
903 hummocky moraine arcs (minor transverse ridges). The locations of some MSGL on the down
904 ice sides of high points on ice stream beds is consistent with a groove-ploughing origin for
905 lineations, especially in the case of the megafluting complex at the centre of CAfs_1 which
906 appears as a flat-topped ridge with a grooved summit. During deglaciation the dynamics of the
907 CAIS in particular switched from fast flow/streaming to steady state flow towards a lobate
908 margin, which was subject to changing sub-marginal thermal regimes as recorded by the arcuate

909 bands of MTR Type 1 – 3 ridges and hummocky terrain located between the preglacial divide
910 (Milk River Ridge) and the Bow River catchment.

911 Large scale mapping of the southern limits of the CAIS reveals a complex glacial
912 geomorphology relating to ice stream marginal recession, comprising minor transverse ridges
913 (MTR types 1-3), hummocky terrain (Types 1-3), flutings and meltwater channels/spillways.
914 MTR Type 1 ridges likely originated through glacitectonic thrusting and have been glacial
915 overrun and moderately streamlined. MTR Type 2 sequences are recessional push moraines
916 similar to those developing at modern active temperate glacier snouts. MTR Type 3 ridges
917 document moraine construction by incremental stagnation, because they occur in association
918 with hummocky terrain. This localized close association of the various types of hummocky
919 terrain with push moraine assemblages as well as proglacial permafrost features, indicates that
920 they are not ice stagnation landforms but rather the products of supraglacial controlled
921 deposition on a polythermal ice sheet margin, where the Type 3 hummocks represent former
922 ice-walled lake plains.

923 The ice sheet marginal thermal regime switches indicated by the spatially variable landform
924 assemblages in southern Alberta are consistent with palaeoglaciological reconstructions
925 proposed for other ice stream lobate margins of the southern Laurentide Ice Sheet, where
926 alternate cold, polythermal and temperate marginal conditions sequentially gave way to more
927 dynamic and surging activity. The sequential south to north change from hummocky terrain to
928 MTR Type 2 to MTR Type 3 within the Lethbridge Moraine and on the northern slopes of the
929 Milk River ridge records a temporal switch in CAIS marginal characteristics, from cold
930 polythermal to temperate and then to warm polythermal. This is similar to patterns previously
931 identified for the HPIS at approximately the same time based upon the available regional
932 morphochronology and hence indicates a potential regional climatic control on ice sheet
933 marginal activity. To the north of the Lethbridge Moraine, the landform assemblage of the Bow
934 and Red Deer river basins, comprising overridden thrust moraines, megaflutings (CAfs_1) and a
935 fluted esker complex lying inboard of the Vauxhall Ridge, records a later fast flow/streaming

936 event. This was the precursor to the later ice stream surges that constructed the large thrust
937 moraines TR_3 and TR_4 and other surge-diagnostic landforms in central Alberta.

938

939 **Acknowledgements**

940 Research in Alberta has been funded over a number of years by The Royal Society and the
941 Carnegie Trust. Chris Orton, Department of Geography, Durham University drafted the figures.

942

943 **References**

944 Aartolahti, T., 1974. Ring ridge hummocky moraines in northern Finland. *Fennia* 134, 1–21.

945 Aber, J.S., Ber, A., 2007. *Glaciotectonism. Developments in Quaternary Science* 6. Elsevier,
946 London.

947 Aber, J.S., Croot, D.G., Fenton, M.M., 1989. *Glaciotectonic landforms and structures*. Kluwer
948 Academic, Boston.

949 Alley, R.B., 1991. Deforming-bed origin for southern Laurentide till sheets? *Journal of*
950 *Glaciology* 37, 67-76.

951 Alley, R.B., 1993. In search of ice-stream sticky spots. *Journal of Glaciology* 39, 447–454.

952 Anandakrishnan, S., Blankenship, D.D., Alley, R.B., Stoffa, P.L., 1998. Influence of subglacial
953 geology on the position of a West Antarctic ice stream from seismic observations. *Nature*
954 394, 62-66.

955 Attig, J.W., 1993. Pleistocene geology of Taylor County, Wisconsin. *Wisconsin Geological and*
956 *Natural History Survey Bulletin* 90.

957 Attig, J.W., Clayton, Lee, Johnson, M.D., Patterson, C.J., Ham, N.R., Syverson, K.M., 2003.
958 Ice-walled-lake plains in the mid-continent - what they tell us about late glacial ice marginal
959 processes and environments. *Geological Society of America Program and Abstracts* 35, 61.

960 Bamber, J.L., Ferraccioli, F., Joughin, I., Shepherd, T., Rippin, D.M., Siegert, M.J., Vaughan,
961 D.G. 2006. East Antarctic ice stream tributary underlain by a major sedimentary basin.
962 *Geology* 34, 33-36.

963 Bauder, A., Mickelson., D.M., Marshall, S.J., 2005. Numerical modeling investigations of the
964 subglacial conditions of the southern Laurentide ice sheet. *Annals of Glaciology* 40, 219-
965 224.

966 Beaney, C.L., 2002. Tunnel channels in southeast Alberta, Canada: evidence for catastrophic
967 channelized drainage. *Quaternary International* 90, 67-74.

968 Beaney, C.L., Hicks, F.E., 2000. Hydraulic modelling of subglacial tunnel channels, south-east
969 Alberta, Canada. *Hydrological Processes* 14, 2545-2557.

970 Beaney, C.L., Shaw, J., 2000. The subglacial geomorphology of southeast Alberta: evidence for
971 subglacial meltwater erosion. *Canadian Journal of Earth Sciences* 37, 51–61

972 Beaty, C.B., 1990. Milk River in Southern Alberta: A classic underfit stream. *Canadian*
973 *Geographer* 34, 171-174.

974 Bell, R.E., Blankenship, D.D., Finn, C.A., Morse, D.L., Scambos, T.A., Brozena, J.M., Hodge,
975 S.M., 1998. Influence of subglacial geology on the onset of a West Antarctic ice stream from
976 aerogeophysical observations. *Nature* 394, 58–62.

977 Benn, D.I., Evans, D.J.A., 2010. *Glaciers & Glaciation*. Arnold, London.

978 Benn, D.I., Evans, D.J.A., 2006. Subglacial megafloods: outrageous hypothesis or just
979 outrageous? In: Knight, P.G. (Ed.), *Glacier Science and Environmental Change*. Blackwell,
980 Oxford, pp. 42–46.

981 Bennett, G.L., Evans, D.J.A., 2012. Glacier retreat and landform production on an overdeepened
982 glacier foreland: the debris-charged glacial landsystem at Kvíárjökull, Iceland. *Earth Surface*
983 *Processes and Landforms* 37, 1584–1602.

984 Bennett, G.L., Evans, D.J.A., Carbonneau, P., Twigg, D.R., 2010. Evolution of a debris-charged
985 glacier landsystem, Kvíárjökull, Iceland. *Journal of Maps*, 40–67.

986 Bik, M. J. J., 1969. The origin and age of the prairie mounds of southern Alberta, Canada.
987 *Biuletyn Peryglacjalny* 19, 85-130.

988 Bluemle, J.P., 1993. Hydrodynamic blowouts in North Dakota. In: Aber, J.S. (Ed.),
989 *Glaciotectonics and Mapping Glacial Deposits*. Canadian Plains Research Centre, University
990 of Regina, pp. 259-266.

- 1991 Bluemle, J.P., Clayton, L., 1984. Large-scale glacial thrusting and related processes in North
1992 Dakota. *Boreas* 13, 279-299.
- 1993 Bolch, T., Kamp, U., Olsenholler, J., 2005. Using ASTER and SRTM DEMs for studying
1994 geomorphology and glaciations in high mountain areas. In: Oluić, M. (Ed.), *New Strategies*
1995 *for European Remote Sensing*. Millipress, Rotterdam, pp. 119-127.
- 1996 Boone, S.J., Eyles, N., 2001. Geotechnical model for great plains hummocky moraine formed
1997 by till deformation below stagnant ice. *Geomorphology* 38, 109-124.
- 1998 Boulton, G.S., 1967. The development of a complex supraglacial moraine at the margin of
1999 Sørbreen, Ny Friesland, Vestspitsbergen. *Journal of Glaciology* 6, 717-735.
- 1000 Boulton, G.S., 1970. On the origin and transport of englacial debris in Svalbard glaciers. *Journal*
1001 *of Glaciology* 9, 213–229.
- 1002 Boulton, G.S., 1972. Modern arctic glaciers as depositional models for former ice sheets.
1003 *Journal of the Geological Society of London* 128, 361-393.
- 1004 Boulton, G.S., 1986. Push moraines and glacier contact fans in marine and terrestrial
1005 environments. *Sedimentology* 33, 677–698.
- 1006 Boulton, G.S., 1996a. The origin of till sequences by subglacial sediment deformation beneath
1007 mid-latitude ice sheets. *Annals of Glaciology* 22, 75–84.
- 1008 Boulton, G.S., 1996b. Theory of glacier erosion, transport and deposition as a consequence of
1009 subglacial sediment deformation. *Journal of Glaciology* 42, 43–62.
- 1010 Boulton, G.S., Caban, P.E., 1995. Groundwater flow beneath ice sheets: Part II – its impact on
1011 glacier tectonic structures and moraine formation. *Quaternary Science Reviews* 14, 563–587.
- 1012 Canals, M., Urgeles, R., Calafat, A.M., 2000. Deep sea floor evidence of past ice streams off the
1013 Antarctic Peninsula. *Geology* 28, 31-34.
- 1014 Christiansen, E.A., 1979. The Wisconsinan deglaciation of southern Saskatchewan and adjacent
1015 areas. *Canadian Journal of Earth Sciences* 16, 913-938.
- 1016 Clark, C.D., 1999. Glaciodynamic context of subglacial bedform generation and preservation.
1017 *Annals of Glaciology* 28, 23–32.
- 1018 Clark, C.D., Stokes, C.R., 2003. Palaeo-ice stream landsystem. In: Evans, D.J.A. (Ed.), *Glacial*
1019 *Landsystems*. Arnold, London, pp. 204–227.

- 1020 Clark, C.D., Tulaczyk, S.M., Stokes, C.R., Canals, M., 2003. A groove-ploughing theory for the
1021 production of mega scale glacial lineations, and implications for ice-stream mechanics.
1022 *Journal of Glaciology* 49, 240–256.
- 1023 Clark, P.U., 1994. Unstable behaviour of the Laurentide Ice Sheet over deforming sediment and
1024 its implications for climate change. *Quaternary Research* 41, 19-25.
- 1025 Clark, P.U., Licciardi, J.M., MacAyeal, D.R., Jenson, J.W., 1996. Numerical reconstruction of a
1026 soft-bedded Laurentide Ice Sheet during the last glacial maximum. *Geology* 24, 679–682.
- 1027 Clarke, G.K.C., Leverington, D.W., Teller, J.W., Dyke, A.S., Marshall, S.J., 2005. Fresh
1028 arguments against the Shaw megaflood hypothesis. A reply to comments by David Sharpe
1029 on “Paleohydraulics of the last outburst flood from glacial Lake Agassiz and the 8200 BP
1030 cold event”. *Quaternary Science Reviews* 24, 1533-1541.
- 1031 Clayton, L., 1967. Stagnant-glacier features of the Missouri Coteau in North Dakota. North
1032 Dakota Geological Survey, Miscellaneous Series 30, pp. 25-46.
- 1033 Clayton, L., Cherry, J.A., 1967. Pleistocene superglacial and ice walled lakes of west-central
1034 North America. North Dakota Geological Survey Miscellaneous Series 30, pp. 47–52.
- 1035 Clayton, L., Moran, S.R., 1974. A glacial process-form model. In: Coates, D.R. (Ed.), *Glacial*
1036 *Geomorphology*. State University of New York, Binghamton, pp. 89-119.
- 1037 Clayton, L. and Moran, S.R., 1982. Chronology of Late Wisconsinan glaciations in middle
1038 North America. *Quaternary Science Reviews* 1, 55-82.
- 1039 Clayton, L., Attig, J.W., Mickelson, D.M., 2001. Effects of late Pleistocene permafrost on the
1040 landscape of Wisconsin, USA. *Boreas* 30, 173-188.
- 1041 Clayton, L., Attig, J.W., Ham, N.R., Johnson, M.D., Jennings, C.E., Syverson, K.M., 2008. Ice-
1042 walled-lake plains: Implications for the origin of hummocky glacial topography in middle
1043 North America. *Geomorphology* 97, 237–248.
- 1044 Clayton, L., Teller, J.T., Attig, J.W., 1985. Surging of the southwestern part of the Laurentide
1045 Ice Sheet. *Boreas* 14, 235-241.
- 1046 Colgan, P.M., Mickelson, D.M., Cutler, P.M., 2003. Ice marginal terrestrial landsystems:
1047 southern Laurentide ice sheet margin. In: Evans, D.J.A. (Ed.), *Glacial Landsystems*. Arnold,
1048 London, pp. 111-142.

- 1049 Colton, R.B., Lemke, R.W., Lindvall, R.M., 1961. Glacial Map of Montana East of the Rocky
1050 Mountains. U.S. Geological Survey Miscellaneous Investigations Series Map I-327, scale
1051 1:500 000, 1 sheet.
- 1052 Colton, R.B., Fullerton, D.S., 1986. Proglacial lakes along the Laurentide Ice Sheet margin in
1053 Montana. Geological Society of America Abstracts with Programs 18, 347.
- 1054 Davies, N.K., Locke, W.W., Pierce, K.L., Finkel, R.C., 2006. Glacial Lake Musselshell: Late
1055 Wisconsin slackwater on the Laurentide ice margin in central Montana, USA.
1056 *Geomorphology* 75, 330-345.
- 1057 Dyke, A.S., Morris, T.F., 1988. Drumlin fields, dispersal trains and ice streams in arctic Canada.
1058 *Canadian Geographer* 32, 86-90.
- 1059 Dyke, A.S., Prest, V.K., 1987. The Late Wisconsinan and Holocene history of the Laurentide
1060 Ice Sheet. *Geographie physique et Quaternaire* 41, 237-263.
- 1061 Dyke, A.S., Andrews, J.T., Clark, P.U., England, J.H., Miller, G.H., Shaw, J., Veillette, J.J.,
1062 2002. The Laurentide and Innuitian ice sheet during the Last Glacial Maximum. *Quaternary*
1063 *Science Reviews* 21, 9-31.
- 1064 Evans, D.J.A., 1991. A gravel/diamicton lag on the south Albertan prairies, Canada: evidence of
1065 bed armoring in early deglacial sheet-flood/spillway courses. *Geological Society of America*
1066 *Bulletin* 103, 975-982.
- 1067 Evans, D.J.A., 1996. A possible origin for a megafluting complex on the southern Alberta
1068 prairies, Canada. *Zeitschrift für Geomorphologie Suppl. Bd. 106*, 125-148.
- 1069 Evans, D.J.A., 2000. Quaternary geology and geomorphology of the Dinosaur Provincial Park
1070 area and surrounding plains, Alberta, Canada: the identification of former glacial lobes,
1071 drainage diversions and meltwater flood tracks. *Quaternary Science Reviews* 19, 931–958.
- 1072 Evans, D.J.A., 2003. Ice-marginal terrestrial landsystems: active temperate glacier margins. In:
1073 Evans, D.J.A. (Ed.), *Glacial Landsystems*. Arnold, London, pp. 12–43.
- 1074 Evans, D.J.A., 2009. Controlled moraines: origins, characteristics and palaeoglaciological
1075 implications. *Quaternary Science Reviews* 28, 183-208.
- 1076 Evans, D.J.A., 2010. Defending and testing hypotheses: a response to John Shaw’s paper ‘In

1077 defence of the meltwater (megaflood) hypothesis for the formation of subglacial bedform
1078 fields'. *Journal of Quaternary Science* 25, 822–823.

1079 Evans, D.J.A., Campbell, I.A., 1992. Glacial and postglacial stratigraphy of Dinosaur Provincial
1080 Park and surrounding plains, southern Alberta, Canada. *Quaternary Science Reviews* 11,
1081 535–555.

1082 Evans, D.J.A., Campbell, I.A., 1995. Quaternary stratigraphy of the buried valleys of the lower
1083 Red Deer River, Alberta, Canada. *Journal of Quaternary Science* 10, 123–148.

1084 Evans, D.J.A., Hiemstra, J.F., 2005. Till deposition by glacier submarginal, incremental
1085 thickening. *Earth Surface Processes and Landforms* 30, 1633–1662.

1086 Evans, D.J.A., Rea, B.R., 1999. Geomorphology and sedimentology of surging glaciers: a
1087 landsystems approach. *Annals of Glaciology* 28, 75–82.

1088 Evans, D.J.A., Rea, B.R., 2003. Surging glacier landsystem. In: Evans, D.J.A. (Ed.), *Glacial*
1089 *Landsystems*. Arnold, London, pp. 259–288.

1090 Evans, D.J.A., Twigg, D.R., 2002. The active temperate glacial landsystem: a model based on
1091 Breiðamerkurjökull, Iceland. *Quaternary Science Reviews* 21, 2143–2177.

1092 Evans, D.J.A., Clark, C.D., Rea, B.R., 2008. Landform and sediment imprints of fast glacier
1093 flow in the southwest Laurentide Ice Sheet. *Journal of Quaternary Science* 23, 249–272.

1094 Evans, D.J.A., Lemmen, D.S., Rea, B.R., 1999. Glacial landsystems of the southwest
1095 Laurentide Ice Sheet: modern Icelandic analogues. *Journal of Quaternary Science* 14, 673–
1096 691.

1097 Evans, D.J.A., Rea, B.R., Hiemstra, J.F., Ó Cofaigh, C., 2006. A critical assessment of
1098 subglacial mega-floods: a case study of glacial sediments and landforms in south-central
1099 Alberta, Canada. *Quaternary Science Reviews* 25, 1638–1667.

1100 Evans, D.J.A., Twigg, D.R., Rea, B.R., Shand, M., 2007. Surficial geology and geomorphology
1101 of the Brúarjökull surging glacier landsystem. 1:25000 Map/Poster. University of Durham.

1102 Evans, D.J.A., Hiemstra, J.F., Boston, C.M., Leighton, I., Ó Cofaigh, C., Rea, B.R., 2012.
1103 Till stratigraphy and sedimentology at the margins of terrestrially terminating ice streams:
1104 case study of the western Canadian prairies and high plains. *Quaternary Science Reviews* 46,
1105 80–125.

1106 Eyles, N., 1979. Facies of supraglacial sedimentation on Icelandic and alpine temperate glaciers.
1107 Canadian Journal of Earth Scientists 16, 1341-1361.

1108 Eyles, N., 1983. Modern Icelandic glaciers as depositional models for 'hummocky moraine' in
1109 the Scottish Highlands. In: Evenson, E.B. (Ed.), Tills and Related Deposits. Balkema,
1110 Rotterdam, pp. 47-59.

1111 Eyles N., Boyce, J.I., Barendregt, R.W., 1999. Hummocky moraine: sedimentary record of
1112 stagnant Laurentide Ice Sheet lobes resting on soft beds. Sedimentary Geology 123, 163–
1113 174.

1114 Falorni, G., Teles, V., Vivoni, E.R., Bras, R.L., Amaratunga, K.S., 2005. Analysis and
1115 characterization of the vertical accuracy of digital elevation models from the Shuttle Radar
1116 Topography Mission. Journal of Geophysical Research 110, F02005, DOI:
1117 10.1029/2003JF000113, 2005

1118 Fisher, D.A., Reeh, N., Langley, K., 1985. Objective reconstructions of the Late Wisconsinan
1119 Ice Sheet. Géographie Physique et Quaternaire 39, 229-238.

1120 Fisher, T.G., Spooner, I. 1994., Subglacial meltwater origin and subaerial meltwater
1121 modification of drumlins near Morley, Alberta, Canada. Sedimentary Geology 91, 285–298.

1122 Fullerton, D.S., Bush, C.A., Colton, R.B., Straub, A.W., 2004a. Map showing spatial and
1123 temporal relations of mountain and continental glaciations on the northern plains, primarily
1124 in northern Montana and northwestern North Dakota. U.S. Geological Survey Geologic
1125 Investigations Series Map I-2843, scale 1: 1,000,000, 1 sheet with accompanying text.

1126 Fullerton, D.S., Colton, R.B., Bush, C.A., 2004b. Limits of mountain and continental glaciations
1127 east of the Continental Divide in northern Montana and north-western North Dakota, USA.
1128 In: Ehlers, J. and Gibbard, P.L. (eds.), Quaternary Glaciations – Extent and Chronology Part
1129 II: North America, Elsevier, London.

1130 Fulton, R.J., 1995. Surficial Materials of Canada. Map 1880A, Geological Survey of Canada:
1131 Ottawa.

1132 Geiger, R.W., 1967. Bedrock topography of the Gleichen map area, Alberta. Research Council
1133 of Alberta, Report 67-2.

- 1134 Glasser, N.F., Hambrey, M.J., 2003. Ice-marginal terrestrial landsystems: Svalbard polythermal
1135 glaciers. In: Evans, D.J.A. (Ed.), *Glacial Landsystems*. Arnold, London, pp. 65–88.
- 1136 Glasser, N.F., Jansson, K.N., 2005. Fast-flowing outlet glaciers of the Last Glacial Maximum
1137 Patagonian Icefield. *Quaternary Research* 63, 206-211.
- 1138 Gravenor, C.P., Kupsch, W.O., 1959. Ice disintegration features in western Canada. *Journal of*
1139 *Geology* 67, 48–64.
- 1140 Ham, N.R., Attig, J.W., 1996. Ice wastage and landscape evolution along the southern margin of
1141 the Laurentide Ice Sheet, north-central Wisconsin. *Boreas* 25, 171-186.
- 1142 Hambrey, M.J., Huddart, D., Bennett, M.R., Glasser, N.F., 1997. Genesis of ‘hummocky
1143 moraine’ by thrusting in glacier ice: evidence from Svalbard and Britain. *Journal of the*
1144 *Geological Society of London* 154, 623–632.
- 1145 Hambrey, M.J., Bennett, M.R., Dowdeswell, J.A., Glasser, N.F., Huddart, D., 1999. Debris
1146 entrainment and transport in polythermal valley glaciers, Svalbard. *Journal of Glaciology* 45,
1147 69–86.
- 1148 Heyman, J., Hätterstrand, C.H., Stroeven, A.P., 2008. Glacial geomorphology of the Bayan Har
1149 sector of the NE Tibetan Plateau. *Journal of Maps* 2008, 42-62
- 1150 Jackson, L.E., Phillips, F.M., Shimamura, K., Little, E.C., 1997. Cosmogenic ³⁶Cl dating of the
1151 Foothills erratics train, Alberta, Canada. *Geology* 25, 195–198.
- 1152 Jennings, C.E., 2006. Terrestrial ice streams: a view from the lobe. *Geomorphology* 75, 100–
1153 124.
- 1154 Johnson, M.D., Clayton, L., 2003. Supraglacial landsystems in lowland terrain. In: Evans,
1155 D.J.A. (Ed.), *Glacial Landsystems*. Arnold, London, pp. 228-251.
- 1156 Johnson, M.D., Mickelson, D.M., Clayton, L., Attig, J.W., 1995. Composition and genesis of
1157 glacial hummocks, western Wisconsin. *Boreas* 24, 97-116.
- 1158 Joughin, I., Fahnestock, M., MacAyeal, D., Bamber, J.L., Gogineni, P., 2001. Observation and
1159 analysis of ice flow in the largest Greenland ice stream. *Journal of Geophysical Research*
1160 106 (D24) 34, 21–34.
- 1161 Kehew, A.E., Lord, M.L., 1986. Origin and large scale erosional features of glacial lake
1162 spillways in the northern Great Plains. *Geological Society of America Bulletin* 97, 162-177.

1163 Kjaersgaard, A.A., 1976. Reconnaissance soil survey of the Oyen map sheet – 72M
1164 (Preliminary Report). Alberta Institute of Pedology, Report S-76-36.

1165 Klassen, R.W., 1989. Quaternary geology of the southern Canadian Interior Plains. In: Fulton,
1166 R.J. (Ed.), Quaternary Geology of Canada and Greenland, Chapter 2. Geological Survey of
1167 Canada, Geology of Canada, 1 (also Geological Society of America, the Geology of North
1168 America, Vol. K-I).

1169 Knudsen, C.G., Larsen, E., Sejrup, H.P., Stalsberg, K., 2006. Hummocky moraine landscape on
1170 Jæren, SW Norway—implications for glacier dynamics during the last deglaciation.
1171 *Geomorphology* 77, 153 -168.

1172 Kulig, J.J., 1996. The glaciations of the Cypress Hills of Alberta and Saskatchewan and its
1173 regional implications. *Quaternary International* 32, 53-77.

1174 Lagerbäck, R., 1988. The Veiki moraines in northern Sweden widespread evidence of an Early
1175 Weichselian deglaciation. *Boreas* 17, 469–486.

1176 Leckie, D.A., 2006. Tertiary fluvial gravels and evolution of the Western Canadian Prairie
1177 landscape. *Sedimentary Geology* 190, 139-158.

1178 Mollard, J.D., 2000. Ice-shaped ring-forms in western Canada: their airphoto expressions and
1179 manifold polygenetic origins. *Quaternary International* 68, 187–198.

1180 Moran, S.R., Clayton, L., Hooke, R.LeB., Fenton, M.M., Andrashak, L.D., 1980. Glacier-bed
1181 landforms of the Prairie region of North America. *Journal of Glaciology* 25, 457-476.

1182 Munro-stasiuk, M.J., 1999. Evidence for water storage and drainage at the base of the
1183 Laurentide ice-sheet, south-central Alberta, Canada. *Annals of Glaciology* 28, 175-180.

1184 Munro-Stasiuk, M.J., Shaw, J., 1997. Erosional origin of hummocky terrain in south-central
1185 Alberta, Canada. *Geology* 25, 1027-1030.

1186 Munro-Stasiuk, M.J., Shaw, J., 2002. The Blackspring Ridge flute field, south-central Alberta,
1187 Canada: evidence for subglacial sheetflow erosion. *Quaternary International* 90, 75-86.

1188 Munro-Stasiuk, M.J., Sjogren, D., 2006. The erosional origin of hummocky terrain, Alberta,
1189 Canada. In: Knight, P.G. (Ed.), *Glacier Science and Environmental Change*. Blackwell,
1190 Oxford, pp. 33-36.

- 1191 Ó Cofaigh, C., Evans, D.J.A., Smith, R., 2010. Large-scale reorganistaion and sedimentation of
1192 terrestrial ice-streams during a single glacial cycle. *Geological Society of America Bulletin*
1193 122, 743-756.
- 1194 Ó Cofaigh, C., Pudsey, C.J., Dowdeswell, J.A., Morris, P., 2002. Evolution of subglacial
1195 bedforms along a palaeo-ice stream, Antarctic Peninsula continental shelf. *Geophysical*
1196 *Research Letters* 29(8), 10.1029/2001GL014488.
- 1197 Parizek, R.R., 1969. Glacial ice-contact ridges and rings. *Geological Society of America Special*
1198 *Paper* 123, 49–102.
- 1199 Patterson, C.J., 1997. Southern Laurentide ice lobes were created by ice streams: Des Moines
1200 Lobe in Minnesota, USA. *Sedimentary Geology* 111, 249–261.
- 1201 Patterson, C.J., 1998. Laurentide glacial landscapes: the role of ice streams. *Geology* 26, 643–
1202 646.
- 1203 Paul, M.A., 1983. The supraglacial landsystem. In: Eyles, N. (Ed.), *Glacial geology*. Pergamon,
1204 Oxford, pp.71-90.
- 1205 Prest, V.K., Grant, D.R., Rampton, V.N., 1968. *Glacial Map of Canada*. Map 1253A
1206 (1:5000000), Geological Survey of Canada: Ottawa.
- 1207 Price, R.J., 1970. Moraines at Fjallsjökull, Iceland. *Arctic and Alpine Research* 2, 27–42.
- 1208 Price, S.F., Bindschadler, R.A., Hulbe, C.L., Blankenship, D.D., 2002. Force balance along an
1209 inland tributary and onset to Ice Stream D, West Antarctica. *Journal of Glaciology* 48, 20-30.
- 1210 Rabus, B., Eineder, M., Roth, A., Bamler, R., 2003. The shuttle radar topography mission – a
1211 new class of digital elevation models acquired by spaceborne radar. *Journal of*
1212 *Photogrammetry and Remote Sensing* 57, 241-262.
- 1213 Rains, R.B., Shaw, J., Skoye, K.R., Sjogren, D.B., Kvill, D.R., 1993. Late Wisconsin subglacial
1214 megaflood paths in Alberta. *Geology* 21, 323–326.
- 1215 Rains, R.B., Kvill, D., Shaw, J., 1999. Evidence and some implications of coalescent
1216 Cordilleran and Laurentide glacier systems in western Alberta. In: Smith, P.J. (Ed.), *A*
1217 *World of Real Places: Essays in Honour of William C. Wonders*. University of Alberta:
1218 Edmonton, pp. 147–161.

- 1219 Rains, R.B., Shaw, J., Sjogren, D.B., Munro-Stasiuk, M.J., Robert, R., Young, R.R., Thompson,
1220 R.T., 2002. Subglacial tunnel channels, Porcupine Hills, southwest Alberta, Canada.
1221 Quaternary International 90, 57-65.
- 1222 Roberts, D.H., Long, A.J., 2005. Streamlined bedrock terrain and fast ice flow, Jakobshavns
1223 Isbrae, West Greenland: implications for ice stream and ice sheet dynamics. Boreas 34, 25-
1224 42.
- 1225 Roberts, D.H., Yde, J.C., Knudsen, N.T., Long, A.J., Lloyd, J.M., 2009. Ice marginal dynamics
1226 during surge activity, Kuannersuit Glacier, Disko Island, West Greenland. Quaternary
1227 Science Reviews 28, 209-222.
- 1228 Sharp, M.J., 1984. Annual moraine ridges at Skalafellsjökull, southeast Iceland. Journal of
1229 Glaciology 30, 82-93
- 1230 Shaw, J., 2002. The meltwater hypothesis for subglacial bedforms. Quaternary International 90,
1231 5-22.
- 1232 Shaw, J., 2010. In defence of the meltwater (megaflood) hypothesis for the formation of
1233 subglacial bedform fields. Journal of Quaternary Science 25, 249-260.
- 1234 Shaw, J., Rains, R.B., Eyton, J.R., Weissling L., 1996. Laurentide subglacial outburst floods:
1235 landform evidence from digital elevation models. Canadian Journal of Earth Sciences 33,
1236 1154-1168.
- 1237 Shaw, J., Faragini, D., Kvill, D.R., Rains, R.B., 2000. The Athabasca fluting field, Alberta,
1238 Canada: implications for the formation of large scale fluting (erosional lineations).
1239 Quaternary Science Reviews 19, 959-980.
- 1240 Shetsen I., 1984. Application of till pebble lithology to the differentiation of glacial lobes in
1241 southern Alberta. Canadian Journal of Earth Sciences 21, 920-933.
- 1242 Shetsen, I., 1987. Quaternary Geology, Southern Alberta. ARC map (1:500000), Alberta
1243 Research Council: Edmonton, Canada.
- 1244 Shetsen, I., 1990. Quaternary Geology, Central Alberta. ARC map (1:500000), Alberta
1245 Research Council: Edmonton, Canada.

- 1246 Shipp, S.S., Anderson, J.B., Domack, E.W., 1999. Late Pleistocene–Holocene retreat of the
1247 West Antarctic Ice-Sheet system in the Ross Sea: Part 1 – Geophysical results. Geological
1248 Society of America Bulletin 111, 1486-1516.
- 1249 Sjogren, D.B., Rains, R.B., 1995. Glaciofluvial erosional morphology and sediments of the
1250 Coronation-Spondin scabland, east-central Alberta. Canadian Journal of Earth Sciences 32,
1251 565–578.
- 1252 Smith, M. J., Clark, C.D., 2005. Methods for the visualization of digital elevation methods for
1253 landform mapping. Earth Surface Processes and Landforms 30, 885-900.
- 1254 Smith, M.J., Rose, J., Booth, S., 2006. Geomorphological mapping of glacial landforms from
1255 remotely sensed data: An evaluation of the principal data sources and an assessment of the
1256 quality. Geomorphology 76, 148-165.
- 1257 Stalker, A. MacS., 1956. The Erratics Train; Foothills of Alberta. Geological Survey of Canada,
1258 Bulletin 37.
- 1259 Stalker, A. MacS., 1960. Ice-pressed drift forms and associated deposits in Alberta. Geological
1260 Survey of Canada Bulletin 57.
- 1261 Stalker, A. MacS., 1963. Quaternary stratigraphy in southern Alberta. Geological Survey of
1262 Canada, Paper 62-34.
- 1263 Stalker, A. MacS., 1968. Identification of Saskatchewan gravels and sands. Canadian Journal of
1264 Earth Sciences 5, 155-163.
- 1265 Stalker, A. MacS., 1969. Quaternary stratigraphy in southern Alberta. Report II – sections near
1266 Medicine Hat. Geological Survey of Canada, Paper 69-26.
- 1267 Stalker, A. MacS., 1973. The large interdrift bedrock blocks of the Canadian Prairies.
1268 Geological Survey Canada, Paper 75-1A, pp. 421-422
- 1269 Stalker, A. MacS., 1976. Megablocks, or the enormous erratic of the Albertan Prairies.
1270 Geological Survey Canada, Paper 76-1C, pp. 185-188.
- 1271 Stalker, A. MacS., 1977. The probable extent of the Classical Wisconsin ice in southern and
1272 central Alberta. Canadian Journal of Earth Sciences 14, 2614-2619.
- 1273 Stalker, A. MacS., 1983. Quaternary stratigraphy in southern Alberta report 3: the Cameron
1274 Ranch section. Geological Survey of Canada, Paper 83-10.

- 1275 Stalker, A. MacS., Wyder, J.E., 1983. Borehole and outcrop stratigraphy compared with
1276 illustrations from the Medicine Hat area of Alberta. Geological Survey of Canada,
1277 Bulletin, 296.
- 1278 Stokes, C.R., Clark, C.D., 1999. Geomorphological criteria for identifying Pleistocene ice
1279 streams. *Annals of Glaciology* 28, 67–74.
- 1280 Stokes, C.R., Clark, C.D., 2001. Palaeo-ice streams. *Quaternary Science Reviews* 20, 1437–
1281 1457.
- 1282 Stokes, C.R., Clark, C.D., 2002. Are long bedforms indicative of fast ice flow? *Boreas* 31, 239–
1283 249.
- 1284 Stokes, C.R., Clark, C.D., 2003. The Dubawnt Lake palaeo-ice stream: evidence for dynamic
1285 ice sheet behaviour on the Canadian Shield and insights regarding the controls on ice-stream
1286 location and vigour. *Boreas* 32, 263-279.
- 1287 Stokes, C.R., Clark, C.D., Winsborrow, M.C.M., 2006. Subglacial bedform evidence for a
1288 major palaeo-ice stream and its retreat phases in the Amundsen Gulf, Canadian Arctic
1289 Archipelago. *Journal of Quaternary Science* 21, 399-412.
- 1290 Stokes, C.R., Clark, C.D., Olav, B., Lian, O.B., Tulaczyk, S., 2007. Ice stream sticky spots: a
1291 review of their identification and influence beneath contemporary and palaeo-ice streams.
1292 *Earth Science Reviews* 81, 217–249.
- 1293 Storrar, R., Stokes, C.R., 2007. A Glacial Geomorphological Map of Victoria Island, Canadian
1294 Arctic. *Journal of Maps* 2007, 191-210.
- 1295 Strehl, E., 1998. Glazilimnische Kames in Schleswig-Holstein. *Eiszeitalter u. Gegenwart* 48,
1296 19-22.
- 1297 Thomas, G.S.P., Connaughton, M., Dackombe, R.V., 1985. Facies variation in a late Pleistocene
1298 supraglacial outwash sandur from the Isle of Man. *Geological Journal* 20, 193–213.
- 1299 Tsui, P.C., Cruden, D.M., Thomson, S., 1989. Ice thrust terrains and glaciotectionic settings in
1300 central Alberta. *Canadian Journal of Earth Sciences* 26, 1308–1318.
- 1301 Wellner, J.S., Lowe, A.L., Shipp, S.S., Anderson, J.B., 2001. Distribution of glacial geomorphic
1302 features on the Antarctic continental shelf and correlation with substrate. *Journal of*
1303 *Glaciology* 47, 397-411.

1304 Westgate, J.A., 1968. Surficial geology of the Foremost – Cypress Hills area, Alberta. Research
1305 Council of Alberta, Bulletin 22.

1306

1307

1308 **Figure captions**

1309 Figure 1: Location, bedrock topography and palaeo-ice stream maps of the study area: a)

1310 location maps, showing the province of Alberta, Canada and the study area outlined by
1311 two boxes. The larger box covers the area depicted in Figure 3 and the smaller box the
1312 area depicted in Figure 2; b) bedrock topography map, from The Geological Atlas of the
1313 Western Canadian Sedimentary Basin (Alberta Energy and Utilities Board/Alberta
1314 Geological Survey, 1994), including the locations of the CAIS and HPIS ice streams of
1315 Evans et al. (2008). The map highlights the regional NNE dipping slope. The study area
1316 is outlined by two boxes with the larger box representing Figure 3 and the smaller box
1317 representing Figure 2; c) palaeo-ice stream map superimposed on the SRTM imagery of
1318 Alberta and western Saskatchewan, from Ó Cofaigh et al. (2010), with ice stream
1319 activity represented as numbered phases. The CAIS and HPIS are part of the phase 1
1320 activity in the western half of the image; d) location map of the study area depicted in
1321 Figure 2, showing geographical features and place names.

1322 Figure 2: Glacial geomorphology map of southern Alberta based upon the mapping of SRTM
1323 imagery undertaken in this study: a) map of landforms with genetic classifications; b)
1324 map of landforms annotated with place names and the locations of Figures 4-7 & 9-11,
1325 the transverse ridge sets and topographic cross profiles A-E (see Fig. 8).

1326 Figure 3: Flow-sets reconstructed from glacial lineations. Lineations were grouped into flow
1327 sets based primarily on their orientation but also their proximity and location (Clark
1328 1999). Hfs_1-5 relate to the High Plains Ice Stream and CAfs_1 & 2 relate to the
1329 Central Alberta Ice Stream.

1330 Figure 4: SRTM data of transverse ridges situated along the HPIS trunk (TR_1). Note the
1331 streamlined features that make up Hfs_5 to the right of the image and the esker network
1332 in the bottom right corner.

1333 Figure 5: SRTM data of large lobate ridge situated along the CAIS. The Bow River flows
1334 through the centre of the image and the Oldman River along the bottom. Also shown
1335 are TR_6, TR_7 and TR_8, and an esker network situated to the right centre of the
1336 image.

1337 Figure 6: SRTM data of the western section of transverse ridges that cross the entire CAIS
1338 (TR_6, Fig. 2).

1339 Figure 7: SRTM data of the sequence of ridges in the south eastern corner of Alberta (TR_10).
1340 Note the lineations situated just down ice of the ridges (CAfs_2) and the smooth flat
1341 topography in the north west corner representing Pakowki Lake.

1342 Figure 8: Topographic profiles taken from SRTM data (see Figure 2 for location) across the
1343 study area: A) long profile of the bed of the CAIS; B) transverse profile across the beds
1344 of the HPIS and CAIS and the McGregor and Suffield moraine belts; C) transverse
1345 profile across the terrain traversed by the HPIS; D) ice flow parallel profile from
1346 Pakowki Lake across the transverse ridges located on the preglacial drainage divide in
1347 southeastern Alberta; E) transverse profile across the terrain covered by the CAIS
1348 marginal landforms.

1349 Figure 9: Example of hummocky terrain in the McGregor Moraine: a) Landsat ETM+ image of
1350 the moraine assemblage, with McGregor Lake visible as the flat, smooth area in the left
1351 centre and the Little Bow and Bow rivers at the bottom and top of image respectively;
1352 b) larger scale aerial photograph image of the hummocky terrain to the south east of
1353 McGregor Lake, located by the box in Figure 9a.

1354 Figure 10: Flow set Hfs_4 from SRTM data in GeoTIFF format, demonstrating the high level of
1355 spatial coherency and a large esker indicated by white arrows.

1356 Figure 11: Glacial geomorphology map of the landforms produced at the margin of the CAIS.
1357 Black shaded areas represent lakes and ponds, and therefore demarcate the extent of
1358 meltwater channels/spillways and smaller scale depressions between hummocks and
1359 ridges. Minor transverse ridge crests are depicted as black arcuate lines and major
1360 transverse ridges by barbed lines. Flutings are represented by straight lines orientated
1361 oblique to transverse ridges. Black circular symbols represent the largest flat-topped

1362 mounds or ice-walled lake plains. Hatched broken lines depict the margins of major
1363 channels. The typical morphological details of the hummocky terrain, represented here
1364 by densely spaced small scale depressions, are illustrated and summarized in Figures 16
1365 and 17 respectively.

1366 Figure 12: Morphological characteristics of transverse ridge sets within the CAIS marginal
1367 zone. Type 1 ridges are symmetrical in form and have smoothed summits separated by
1368 partially water filled depressions (the dotted line represents the crest of the ridge). Type
1369 2 ridges have sharper crests and vary in wavelength. Type 3 ridges are composed of
1370 numerous strongly orientated hummocks and ridges separated by partially water-filled
1371 depressions with occasional hummocks.

1372 Figure 13: Transverse ridge sets Types 1 and 2 located in the SE corner of the CAIS marginal
1373 Zone and overprinted by lineations. Individual ridge types are identified in a) and c).

1374 Figure 14: Type 2 and 3 ridges: a) aerial photograph mosaic and b) geomorphology map of
1375 Type 2 transverse ridges, located to the east of Pakowki Lake (see Fig. 11). The
1376 northwest corner of the image and map shows Type 3 ridges blending into Type 1
1377 hummocky terrain; c) Type 2 ridges located 5km to the north of image in a) and b)
1378 (centre of image is 49° 23.5' N and 110° 44' W); d) and e) ground views showing the
1379 parallel, smooth crested and discontinuous nature of Type 3 transverse ridges.

1380 Figure 15: Type 3 transverse ridges located in the central portion of the CAIS marginal zone
1381 (see Fig. 11). Individual hummocks and ridge segments are arranged contiguous with
1382 each other, giving rise to linearity in the landform record: a) area located between
1383 Verdigris Coulée and the Milk River; b) area located south of Crow Indian Lake and
1384 Etzikom Coulée.

1385 Figure 16: Examples of Type 1 and 2 hummocks: a) predominantly Type 1 hummocks north of
1386 Pakowki Lake (centre of image is 49° 28' N & 111° 09' W); b) predominantly Type 1
1387 hummocks north of Crow Indian Lake (centre of image is 49° 26' N & 111° 39' W); c)
1388 predominantly Type 2 hummocks north of Pakowki Lake (centre of image is 49° 28' N
1389 & 110° 54.5' W (see also Fig. 21a).

1390 Figure 17: Morphological characteristics of hummocks within the “Lethbridge Moraine”

1391 sequence. The dimensions reflect the largest features in each class.

1392 Figure 18: Examples of hummocky terrain in an aerial photograph mosaic of the area to the east
1393 of Del Bonita, showing the juxtaposition of all 3 hummock types. Also within the image
1394 are the ridges (highlighted by the white arrows) that run through some hummocky
1395 terrain bands. Note that here they run between Type 2 hummocks and in places
1396 constitute parts of the hummock rims (centre of image is 49° 04.5' N & 112° 37' W).

1397 Figure 19: Details of meltwater channels and spillways: a) view eastwards along Etzikom
1398 Coulée; b) aerial photograph extract of the network of channels to the north of Chin
1399 Coulée (centre of image is 49° 37.5' N & 111° 38' W); c) ground view of shallow
1400 channels in the aerial photograph.

1401 Figure 20: Reconstructed palaeoglaciology of the southern Alberta ice streams/lobes during
1402 deglaciation based on published chronologies (Westgate 1968; Clayton & Moran 1982;
1403 Dyke & Prest 1987; Kulig 1996) and constrained by geomorphology presented in this
1404 paper: a) Pakowki advance limit around 14-13.5ka BP; b) Etzikom limit located along
1405 the Lethbridge moraine at around 12.3ka BP; c) Oldman limit at approximately 12ka
1406 BP; d) Vauxhall limit tentatively dated at around 11.7ka BP. The reconstructed position
1407 of the HPIS is based solely on geomorphology and so the chronology of the marginal
1408 positions is speculative. The proglacial lakes are minimal reconstructions based upon
1409 previous work by Westgate (1968), Shetsen (1987) and Evans (2000).

1410 Figure 21: Ice stream marginal end moraine zonation/landsystem model: a) aerial photograph
1411 mosaic of the area to the north of Pakowki Lake, showing the gradation from Type 2
1412 ridges in the southeast corner of the image, through Type 1 to Type 3 and then to
1413 hummocky moraine with intermittent bands of Type 3 in a northwesterly direction; b)
1414 conceptual model of the continuum of landforms created by terrestrial ice stream
1415 margins based primarily on the CAIS case study. Active recessional push moraines
1416 (Types 1 & 2 ridges) document temperate snout conditions during which the lobate ice
1417 stream margin responded to seasonal climate drivers. Fluted terrain containing well
1418 developed esker networks were active at these times. Hummocky moraine arcs
1419 containing ice-walled lake plains, kame mounds and short esker segments represent

1420 cold-based lobe margins when controlled moraine was constructed by widespread
1421 freeze-on and stacking of basal debris rich ice sequences. Between these two ends of the
1422 landform continuum lie moraine arcs composed of aligned hummocks and ponds (Type
1423 3 ridges), indicative of polythermal margins that probably responded to intermediate
1424 timescale (decadal) climate drivers. During later stages of recession, the margin of the
1425 CAIS underwent surging, as documented by the surging landsystem signature in areas
1426 to the north of the study area by Evans et al. (1999, 2008).
1427

Table 1: Data showing the specific characteristics of the flow-sets, which in turn act as a device to help differentiate between particular flow sets.

Flow set	Number of lineations	Mean length (km)	Mean direction (°)	Flow set area (km ²)
Hfs_1	81	1.56	224	702
Hfs_2	110	3.42	141	3162
Hfs_3	66	2.34	119	1631
Hfs_4	260	3.58	170	4150
Hfs_5	147	3.52	160	5964
CAfs_1	30	10	182	6154
CAfs_2	20	4.17	118	849

Table 2: Palaeo-ice stream criteria of the CAIS and HPIS compared to the schema proposed by Stokes and Clark (1999, 2001).

Ice Stream Geomorphological Criteria (Stokes and Clark, 1999, 2001)	CAIS	HPIS
1. Characteristic shape and Dimensions	YES	YES
2. Highly convergent flow patterns	Unknown	NO
3. Highly attenuated bedforms	YES	YES
4. Boothia type erratic dispersal train	YES	YES
5. Abrupt lateral margins	YES	NO
6. Ice stream marginal moraines	YES	YES
7. Glaciotectonic and geotechnical evidence of pervasively deformed till	YES	YES
8. Submarine till delta or sediment fan (trough-mouth fan)	NA*	NA*

* large arcuate assemblages of moraines and thick, complex sequences of tills and associated glacial sediments reported at the former HPIS and CAIS margins by Evans et al. (2008, 2012) are likely to be the terrestrial equivalents of trough-mouth fans.

Figure 1a

[Click here to download high resolution image](#)



Figure 1b
[Click here to download high resolution image](#)

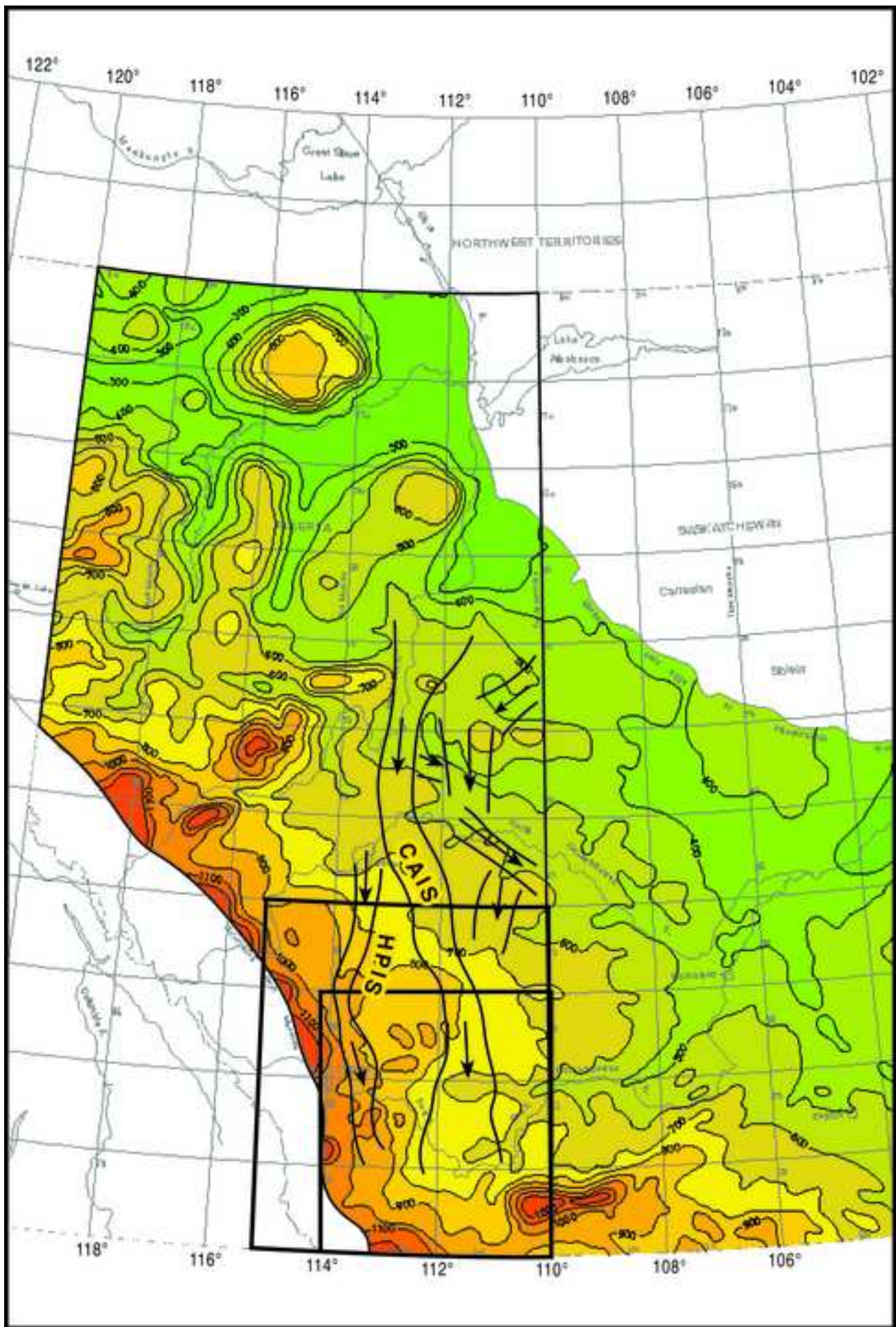


Figure 1c
[Click here to download high resolution image](#)

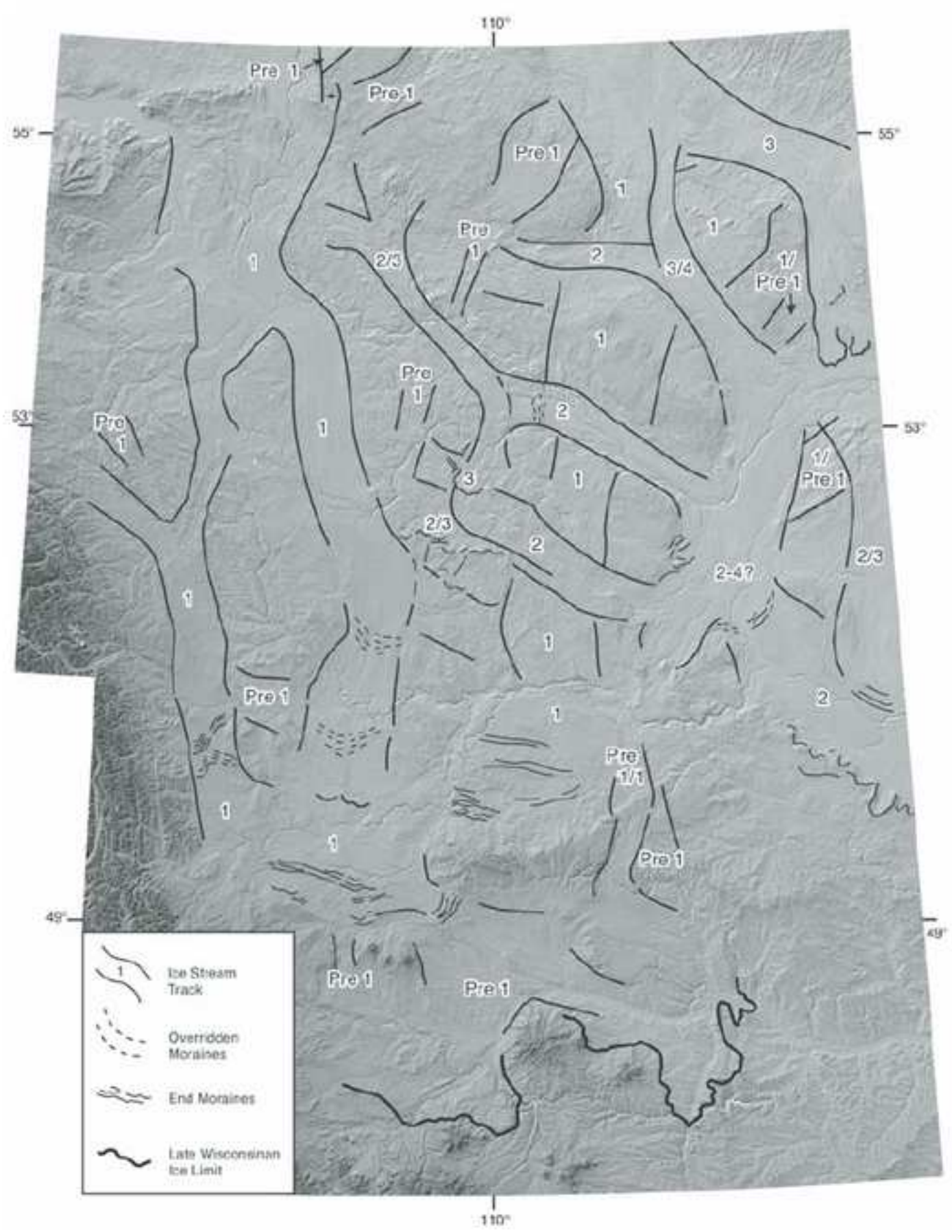


Figure 2a

[Click here to download high resolution image](#)

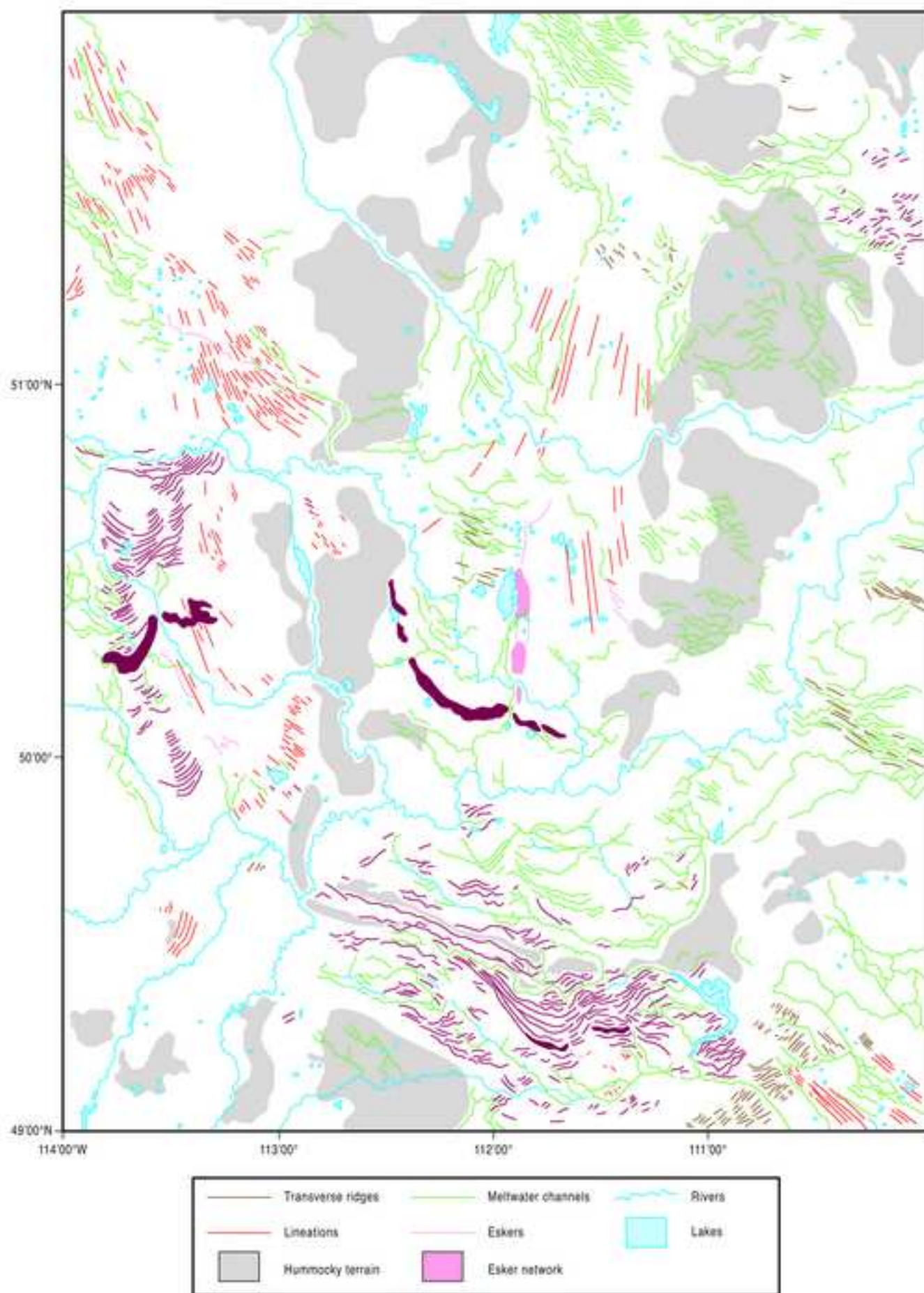


Figure 2b
[Click here to download high resolution image](#)

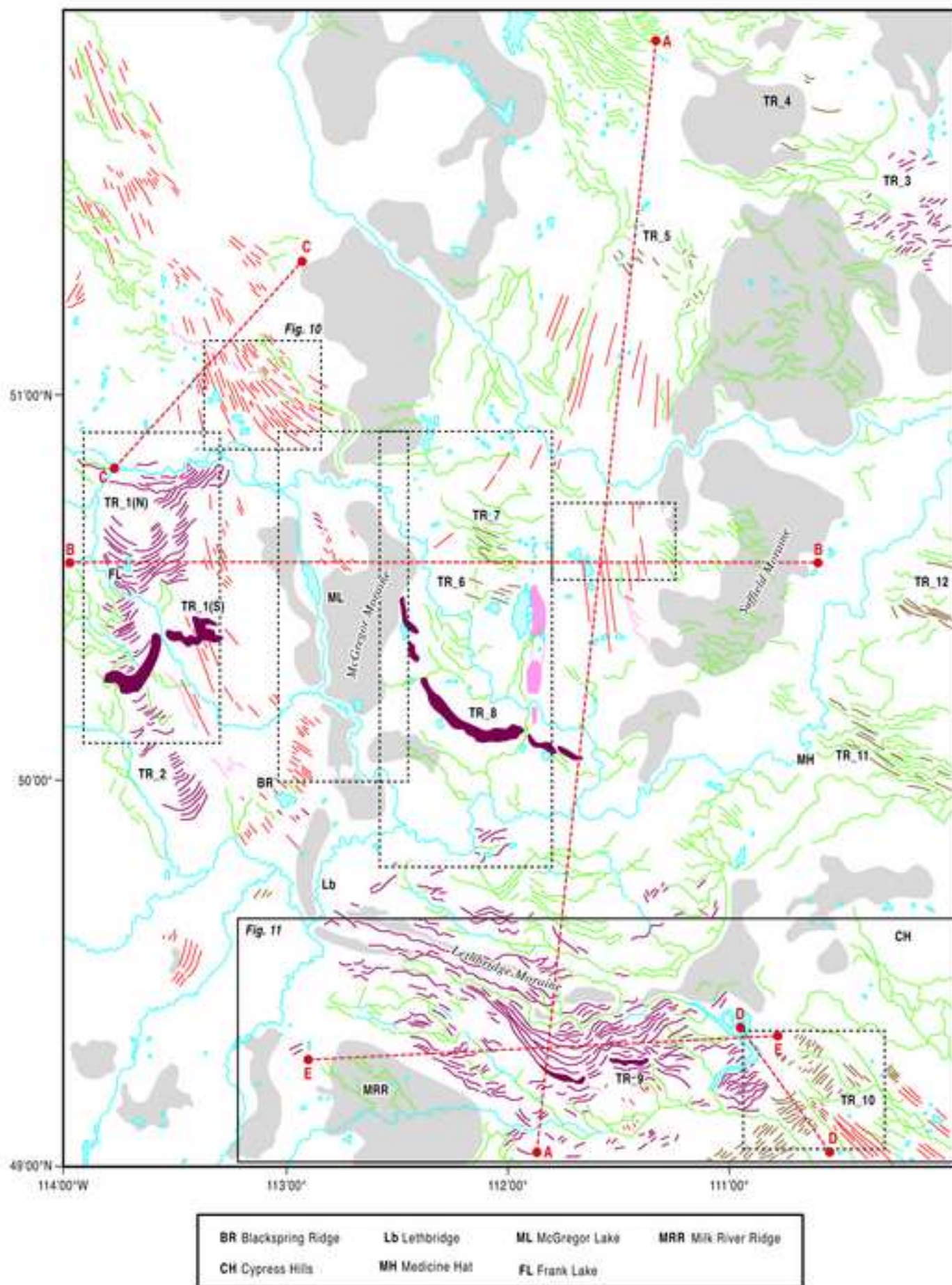


Figure 3
[Click here to download high resolution image](#)

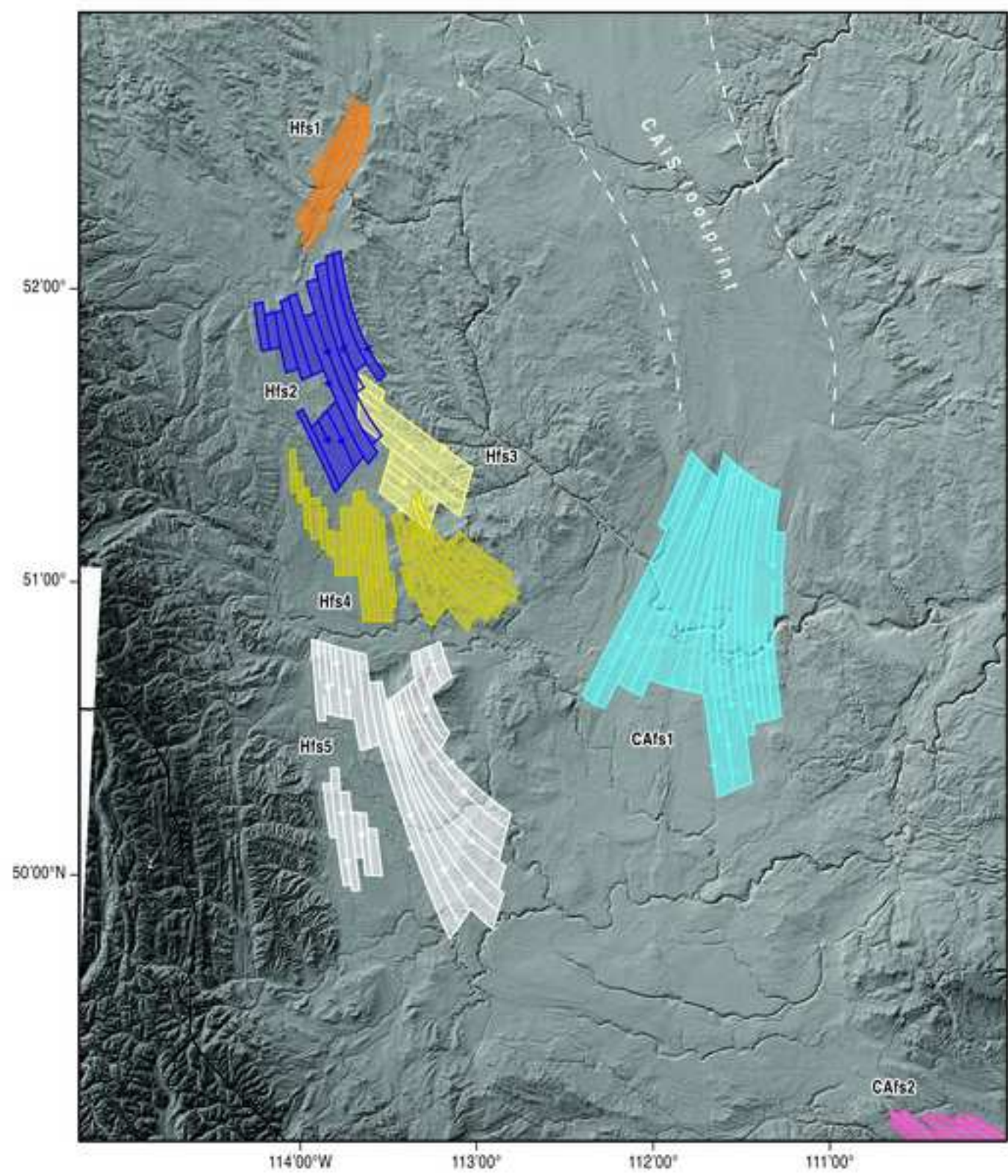


Figure 4

[Click here to download high resolution image](#)

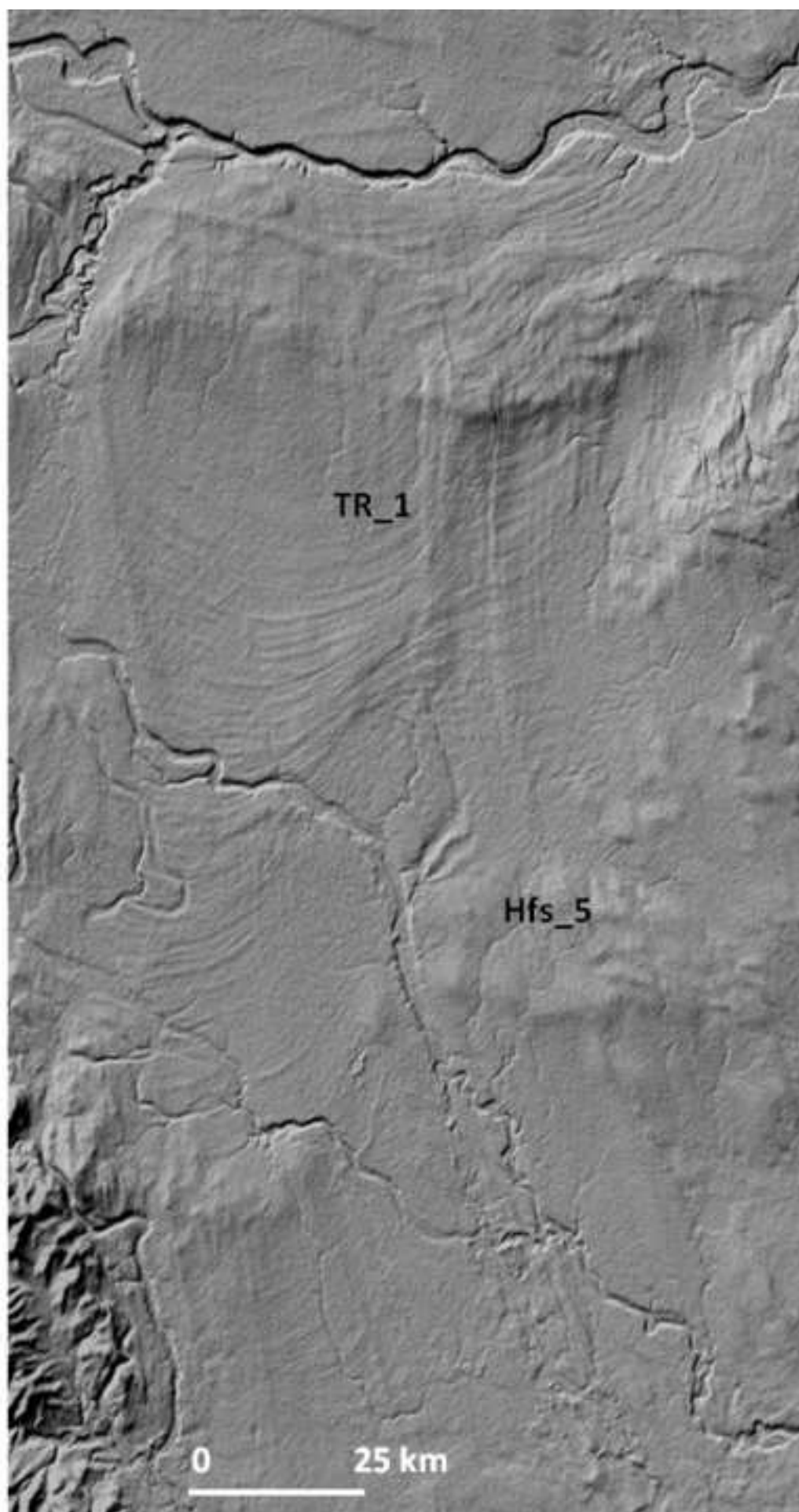


Figure 5
[Click here to download high resolution image](#)

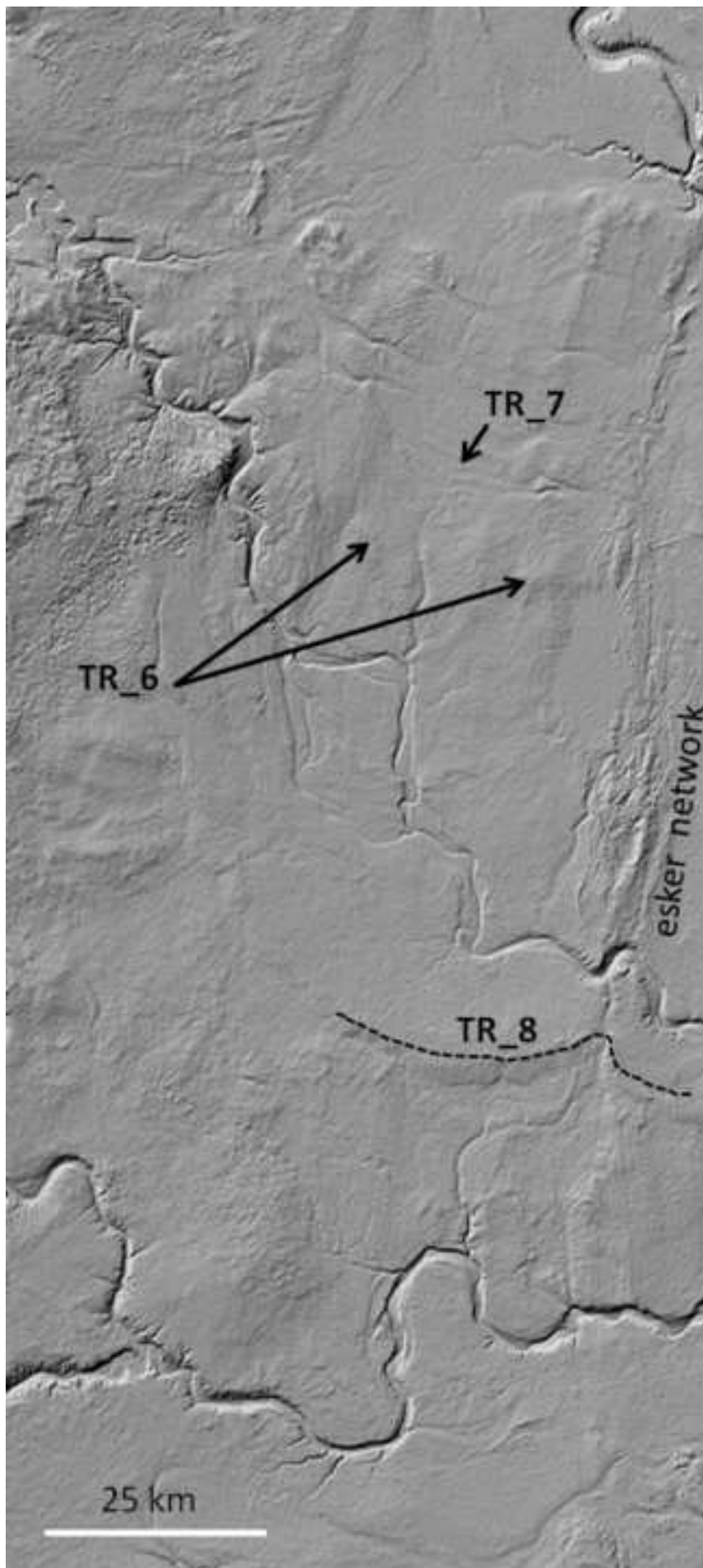


Figure 6
[Click here to download high resolution image](#)

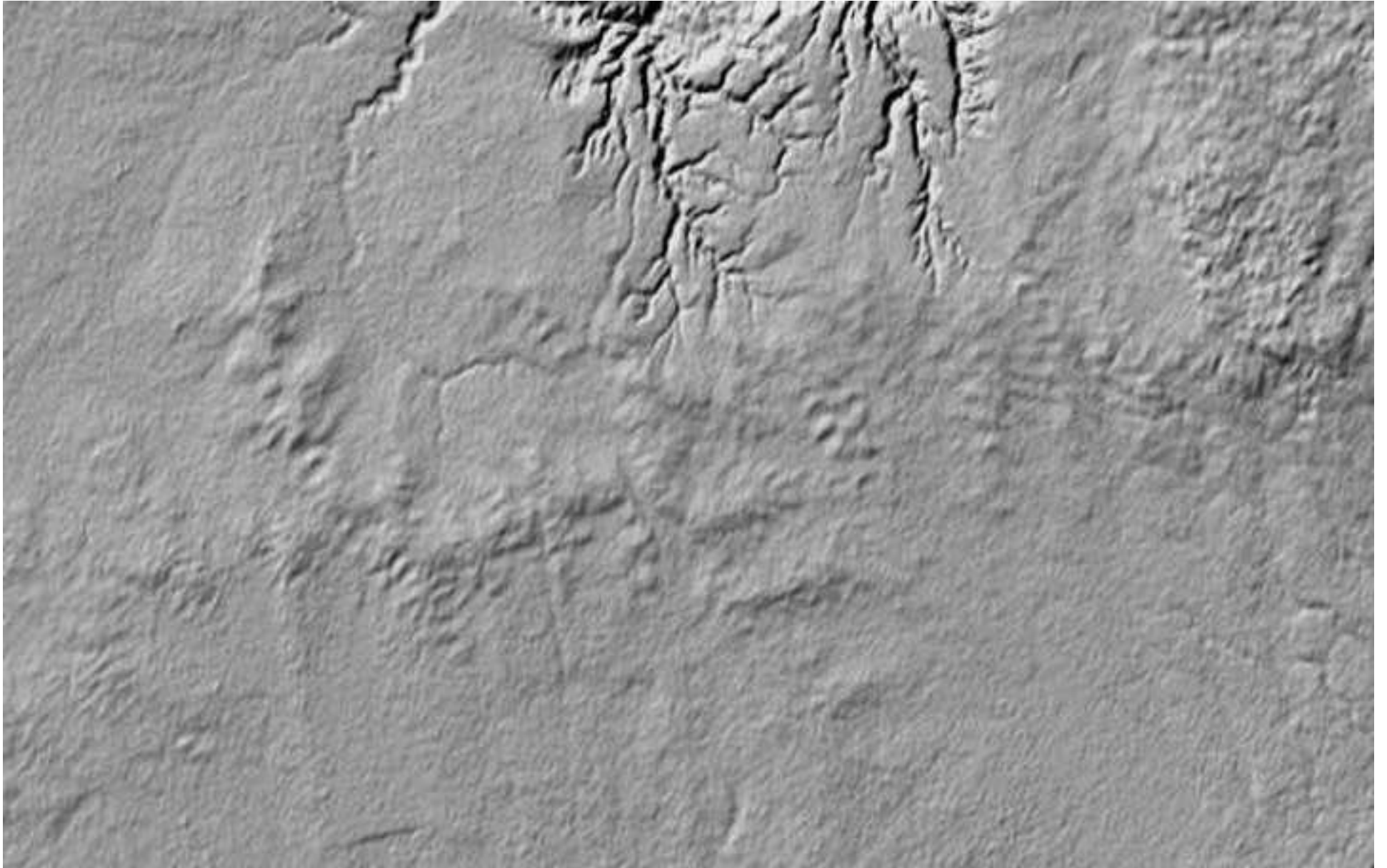


Figure 7
[Click here to download high resolution image](#)

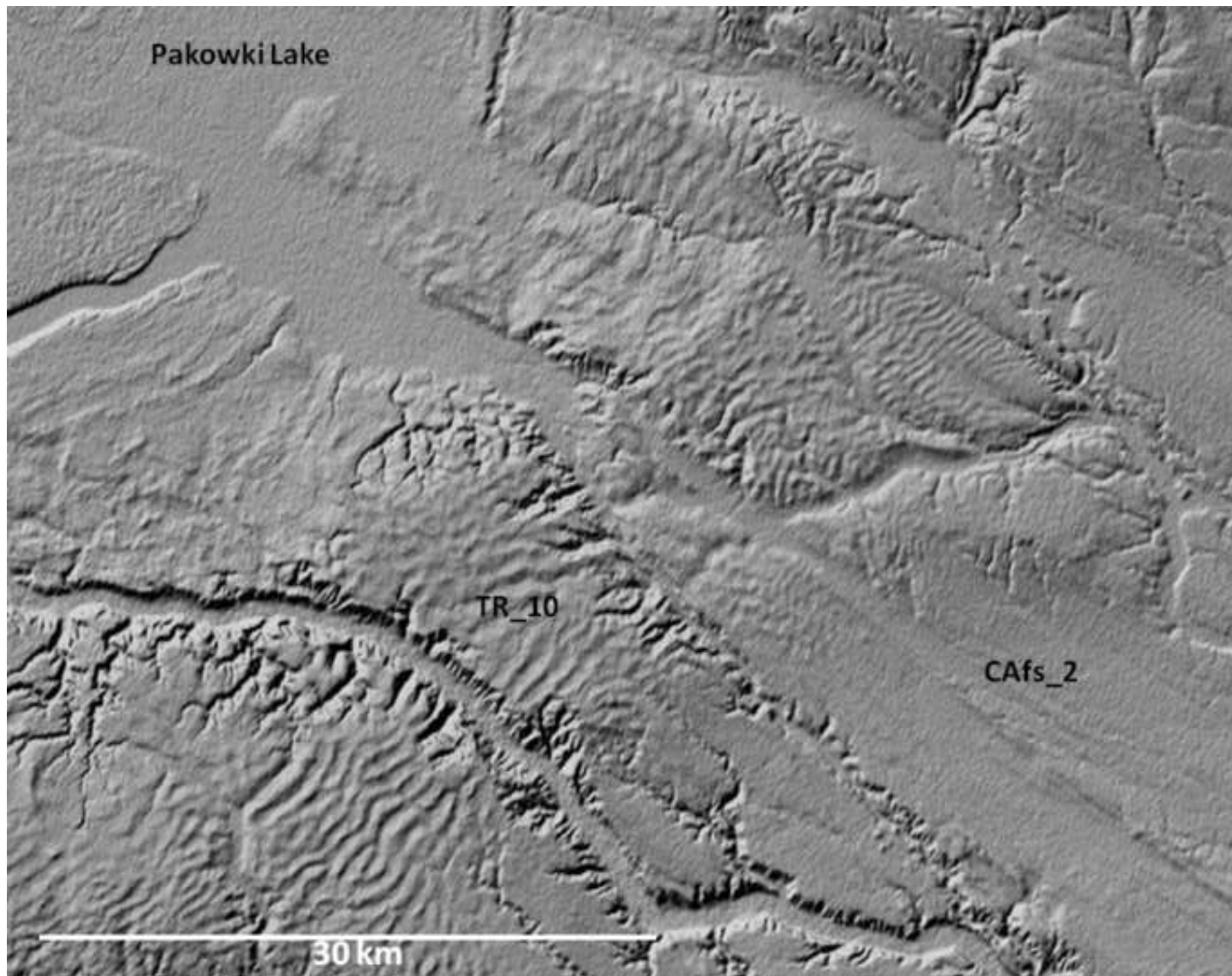


Figure 8
[Click here to download high resolution image](#)

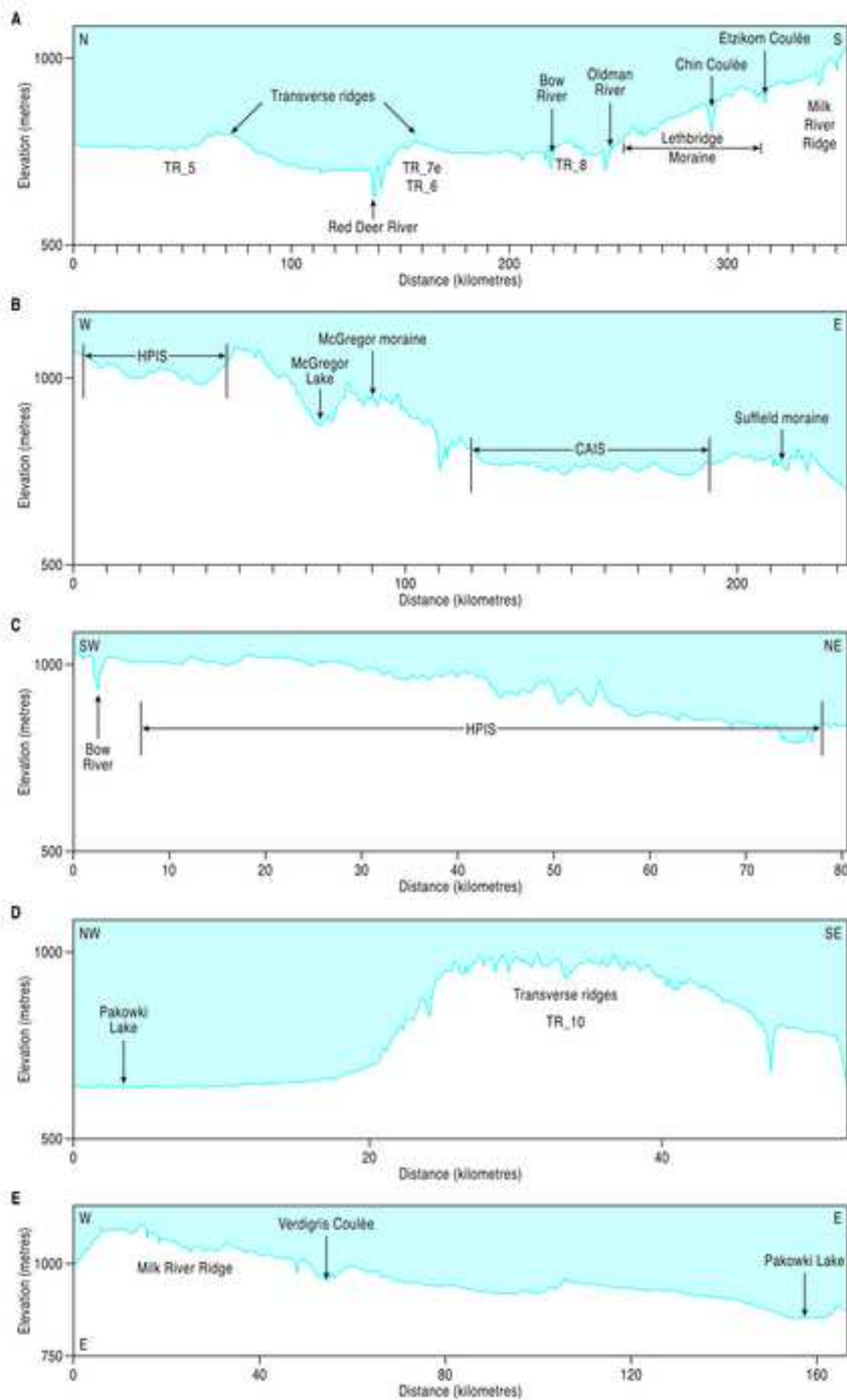


Figure 9a

[Click here to download high resolution image](#)

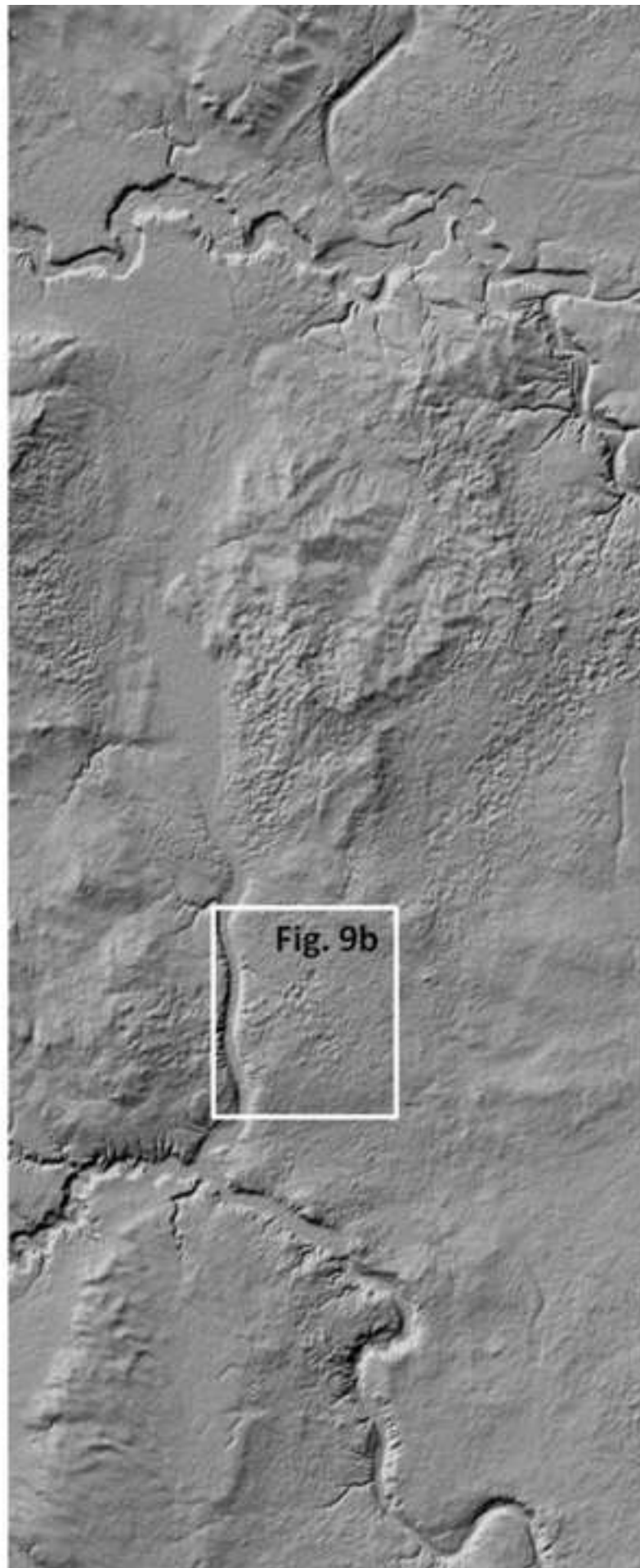


Figure 9b
[Click here to download high resolution image](#)

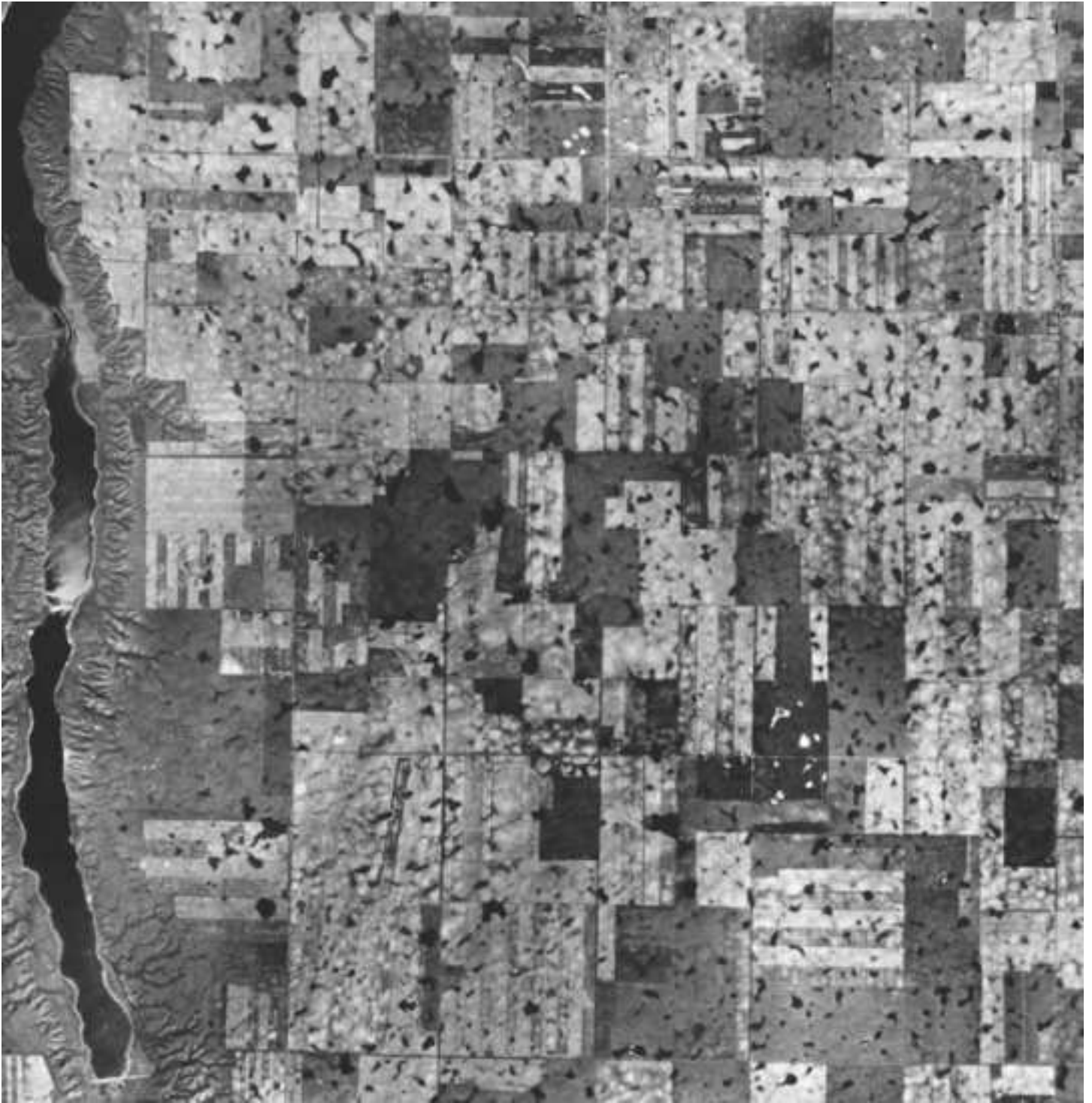


Figure 10
[Click here to download high resolution image](#)

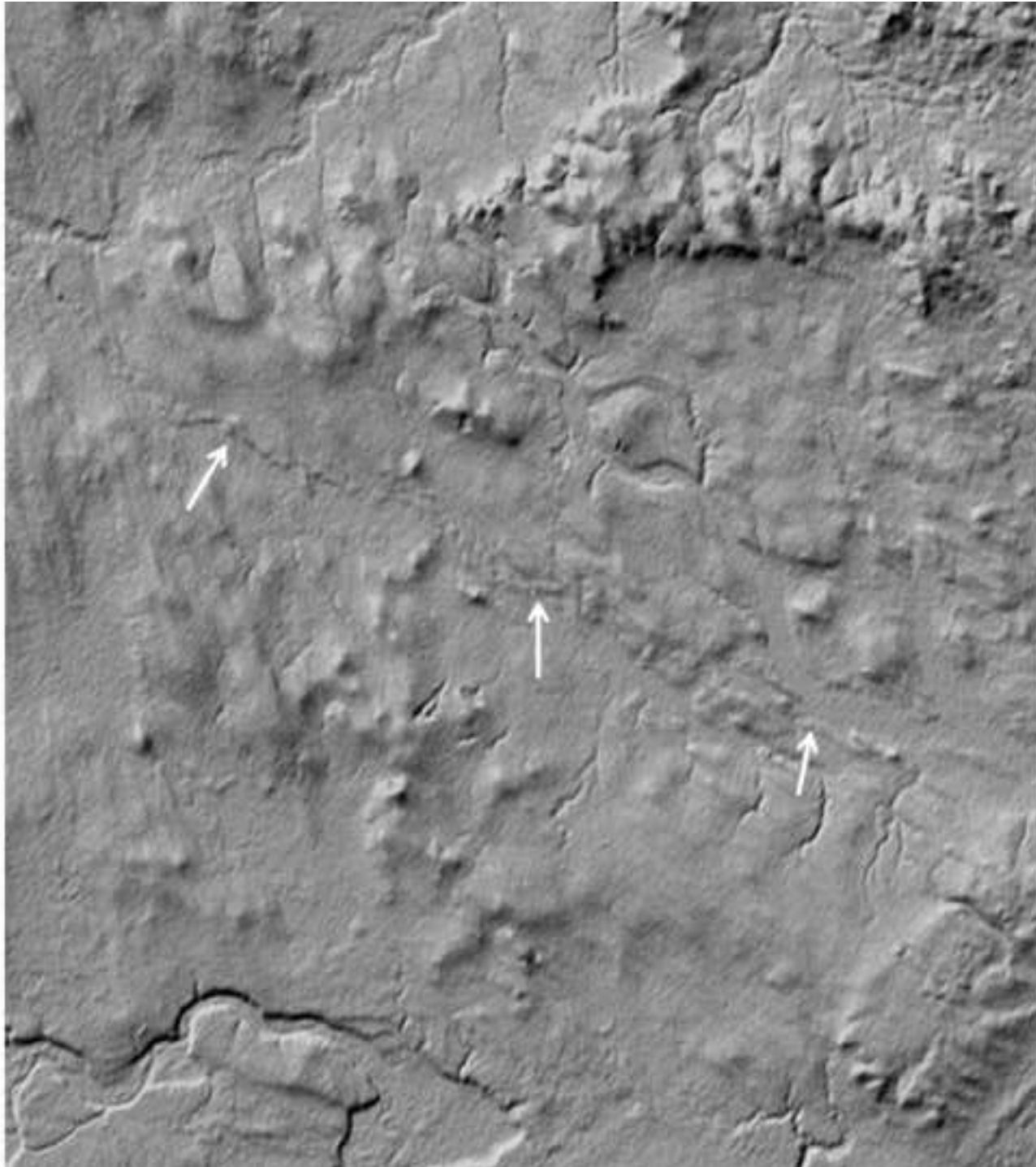


Figure 11
[Click here to download high resolution image](#)

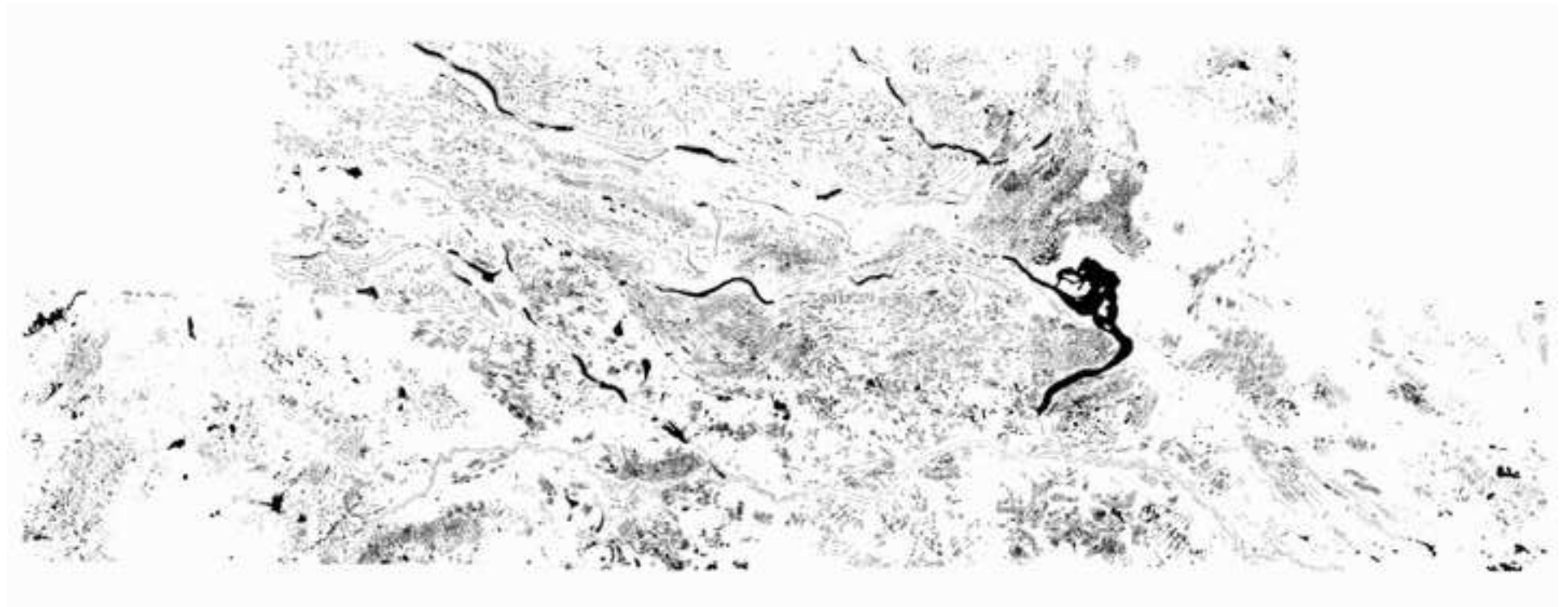


Figure 12
[Click here to download high resolution image](#)

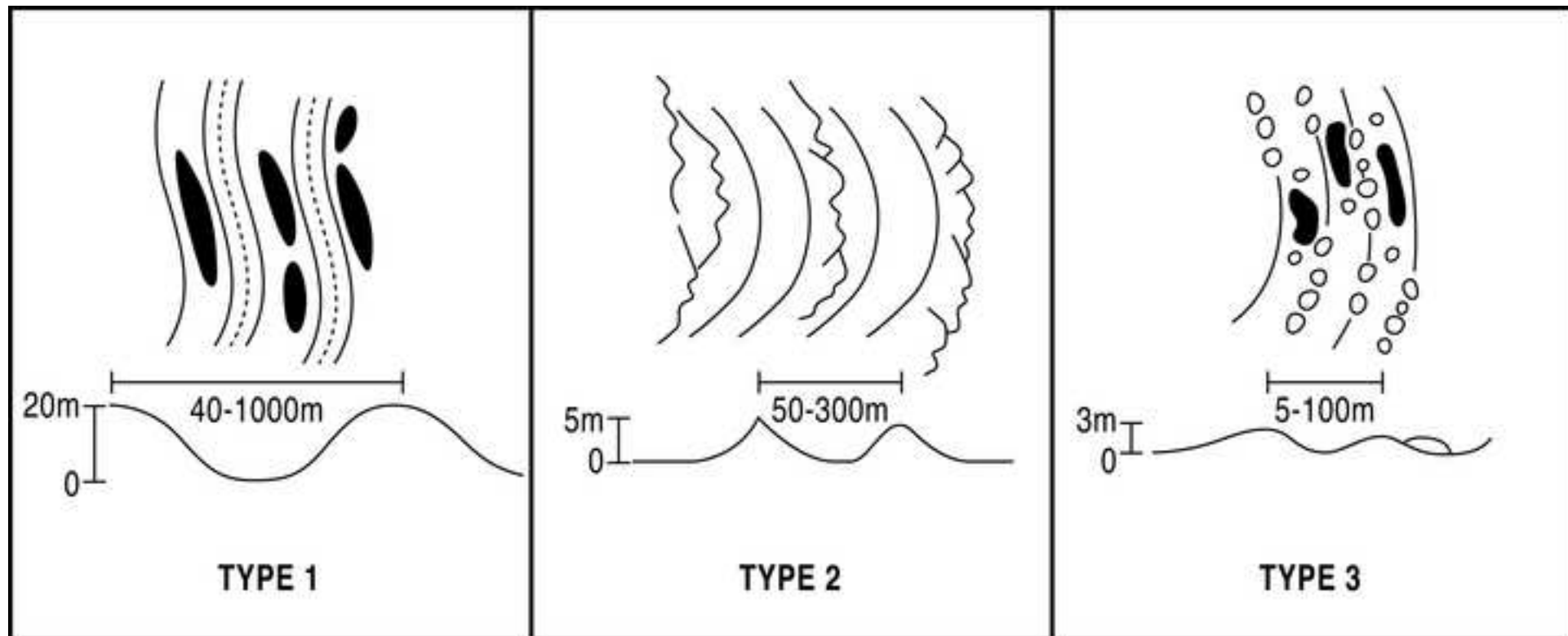


Figure 13
[Click here to download high resolution image](#)

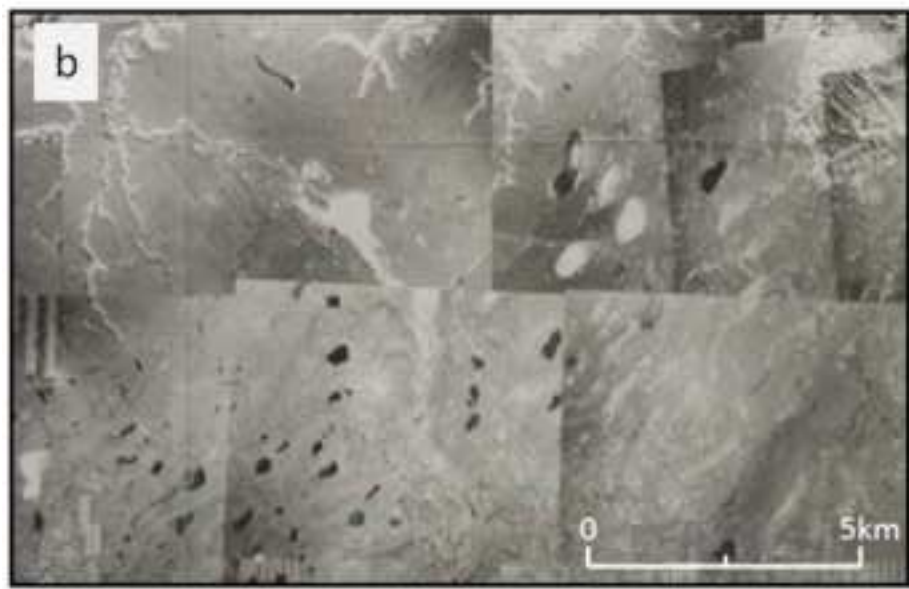
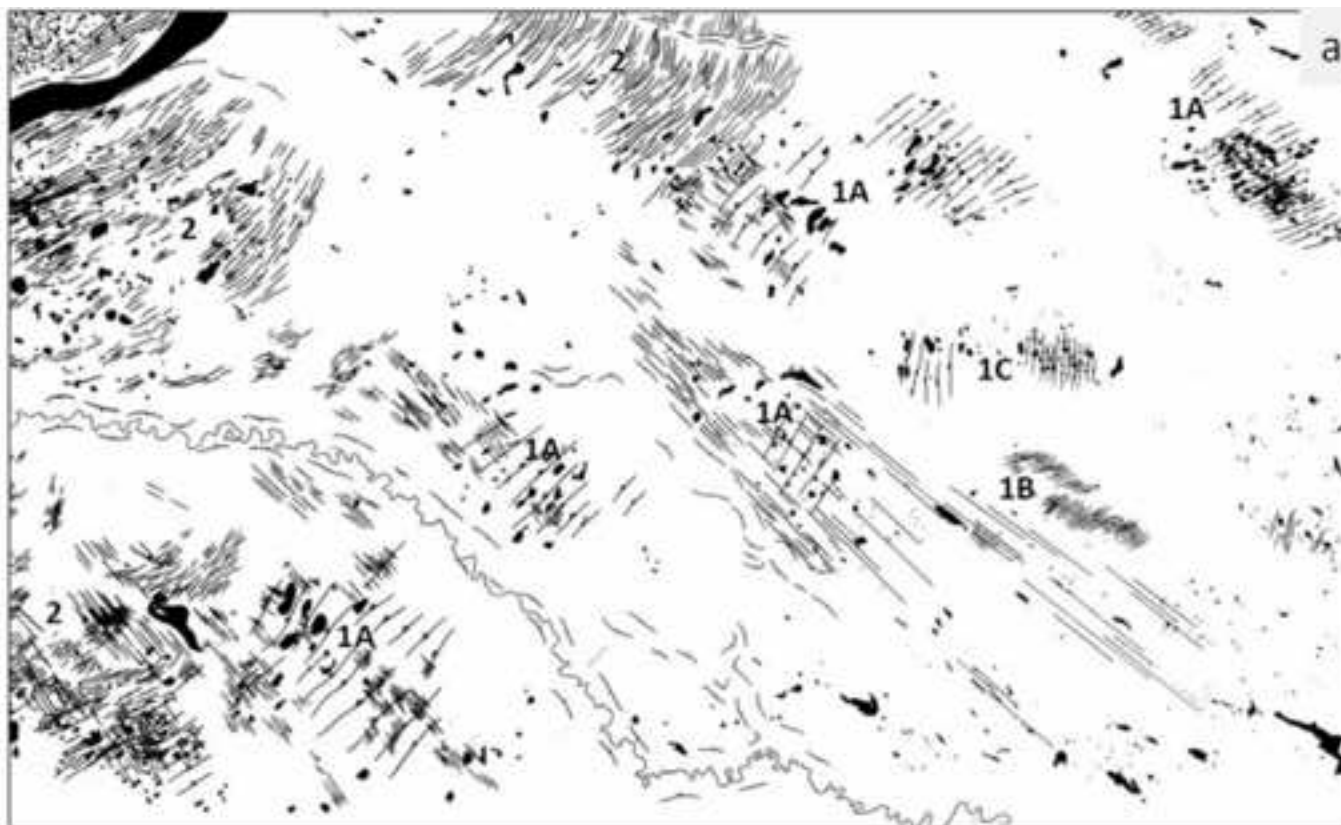


Figure 14
[Click here to download high resolution image](#)

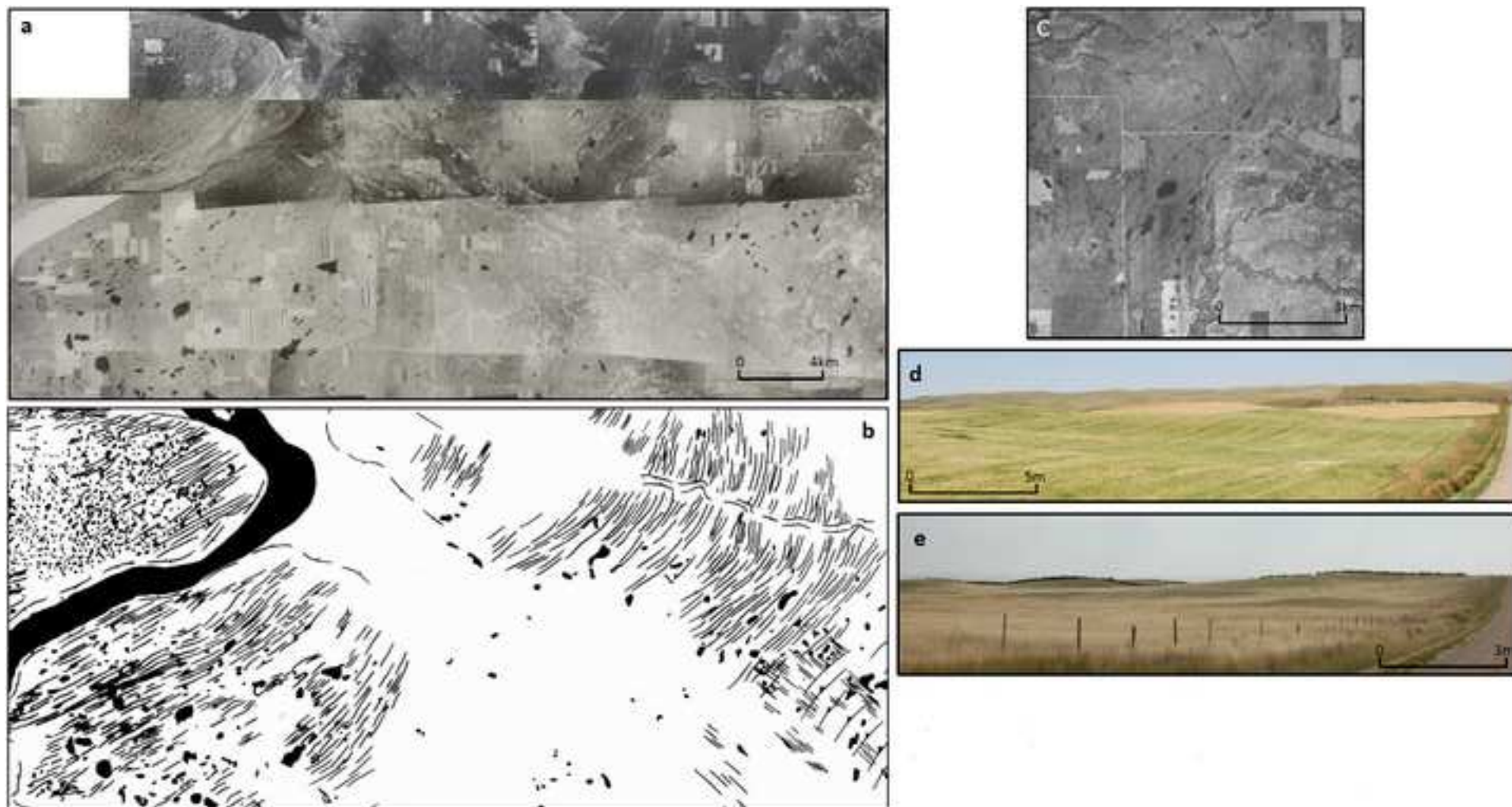


Figure 15

[Click here to download high resolution image](#)

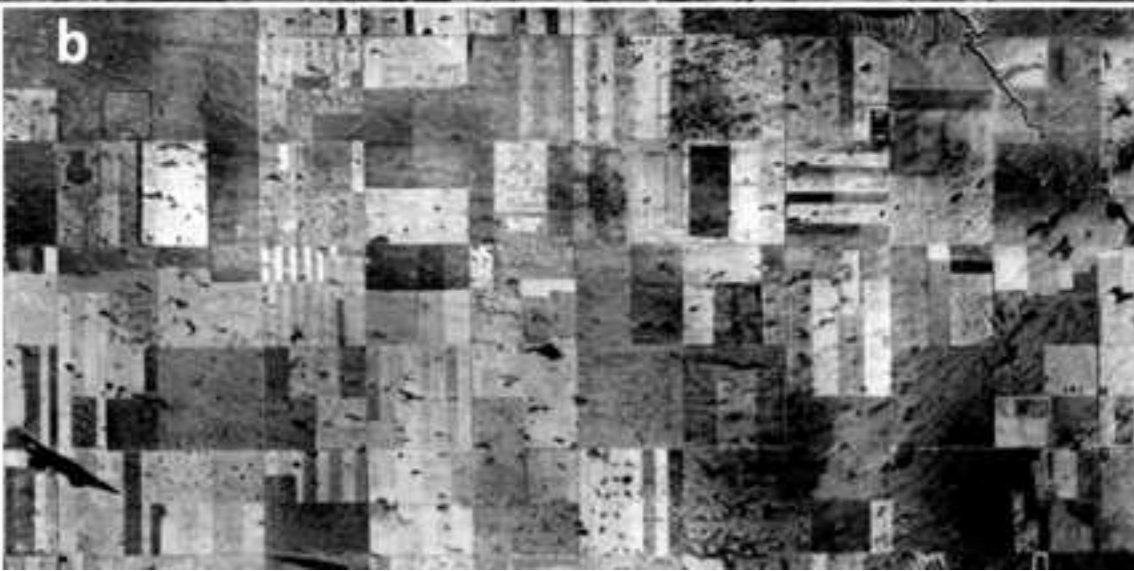
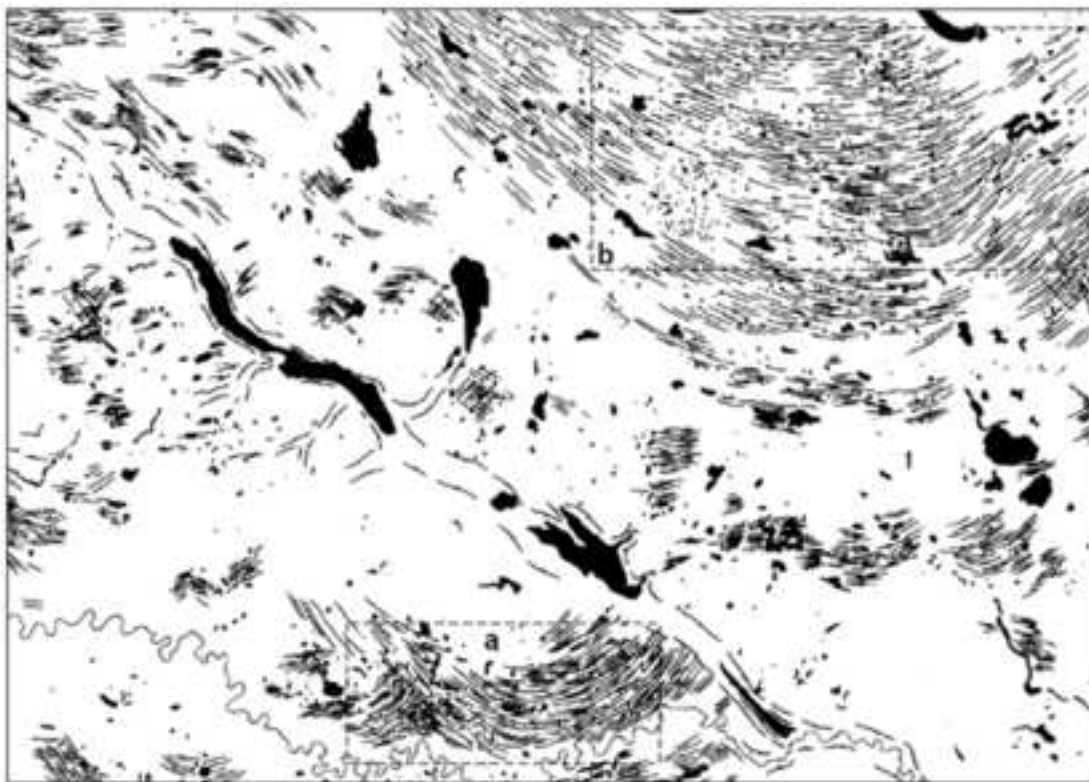


Figure 16
[Click here to download high resolution image](#)

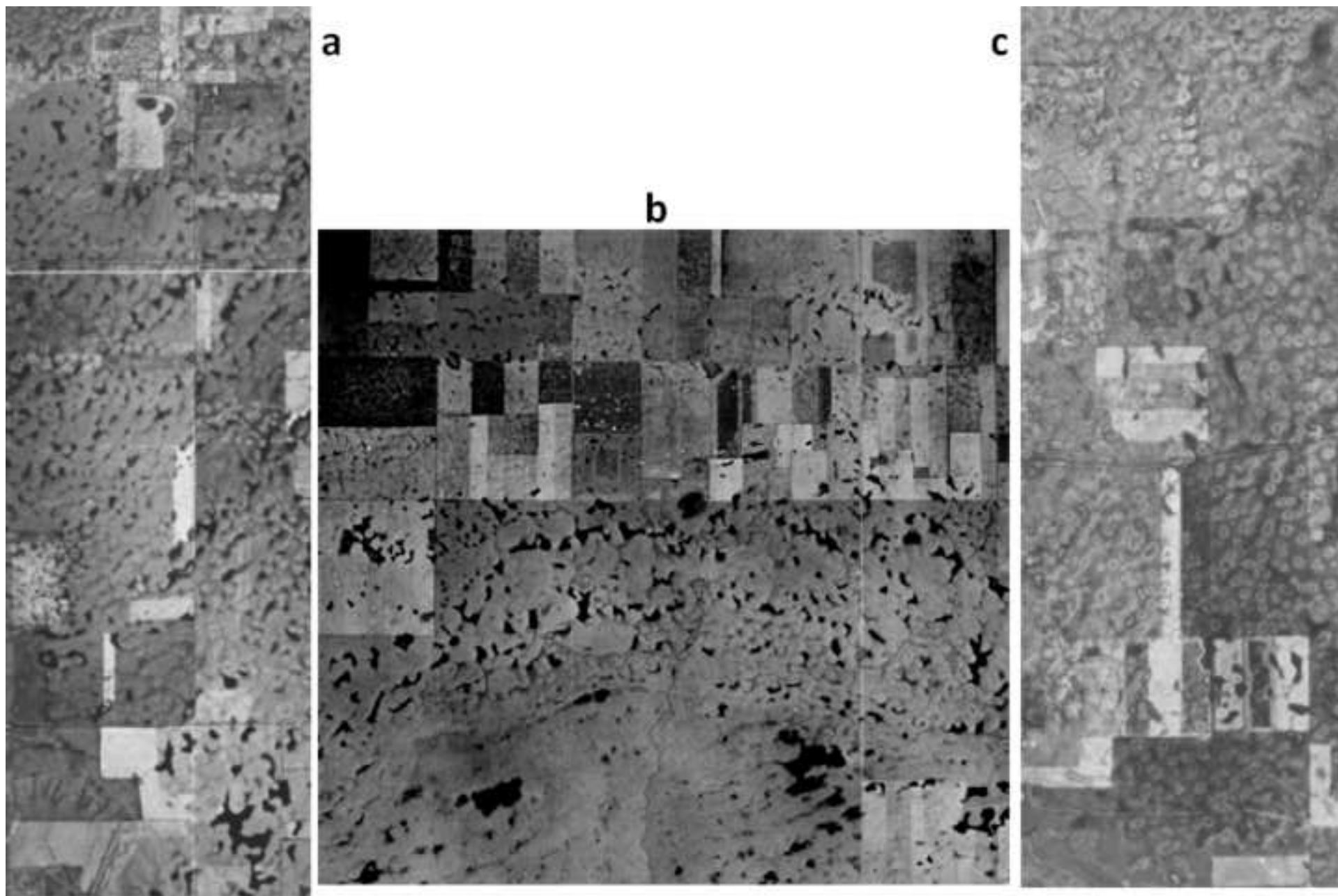


Figure 17
[Click here to download high resolution image](#)

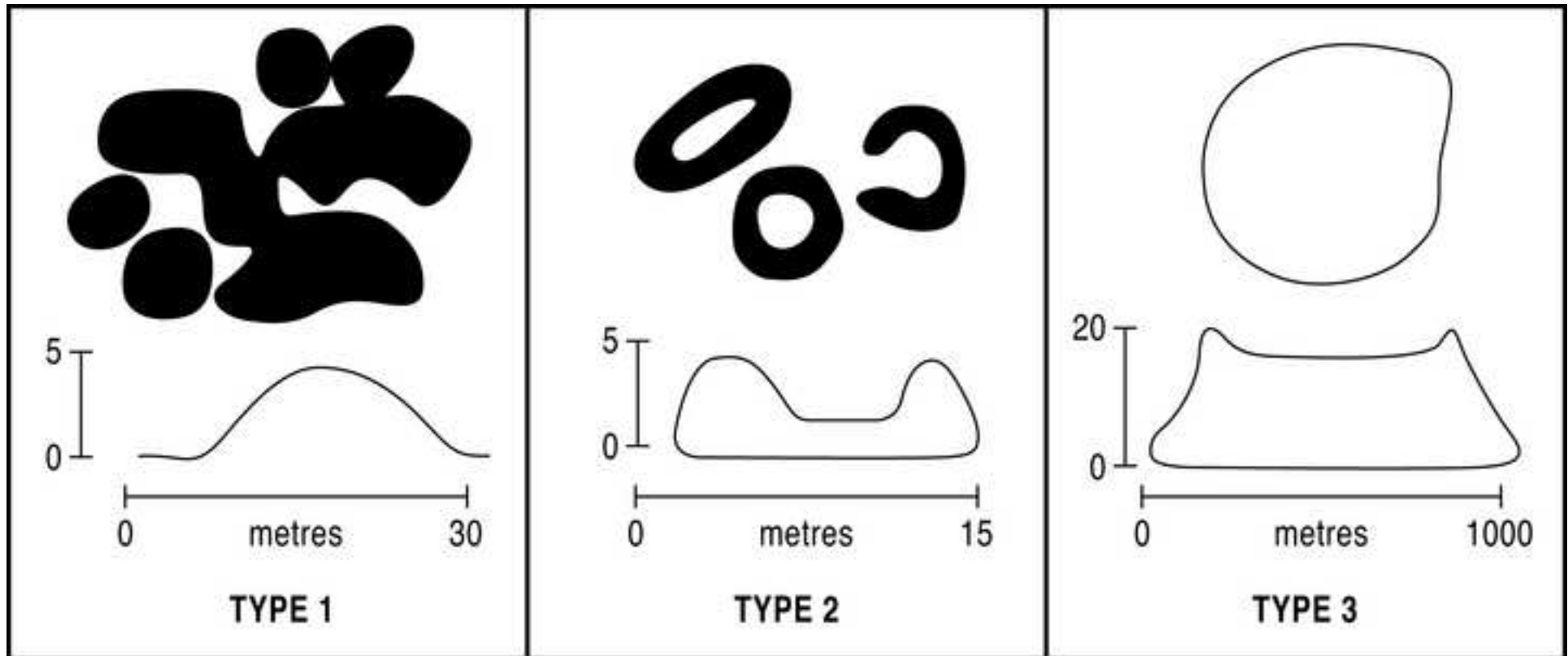


Figure 18
[Click here to download high resolution image](#)



Figure 19
[Click here to download high resolution image](#)



Figure 20

[Click here to download high resolution image](#)

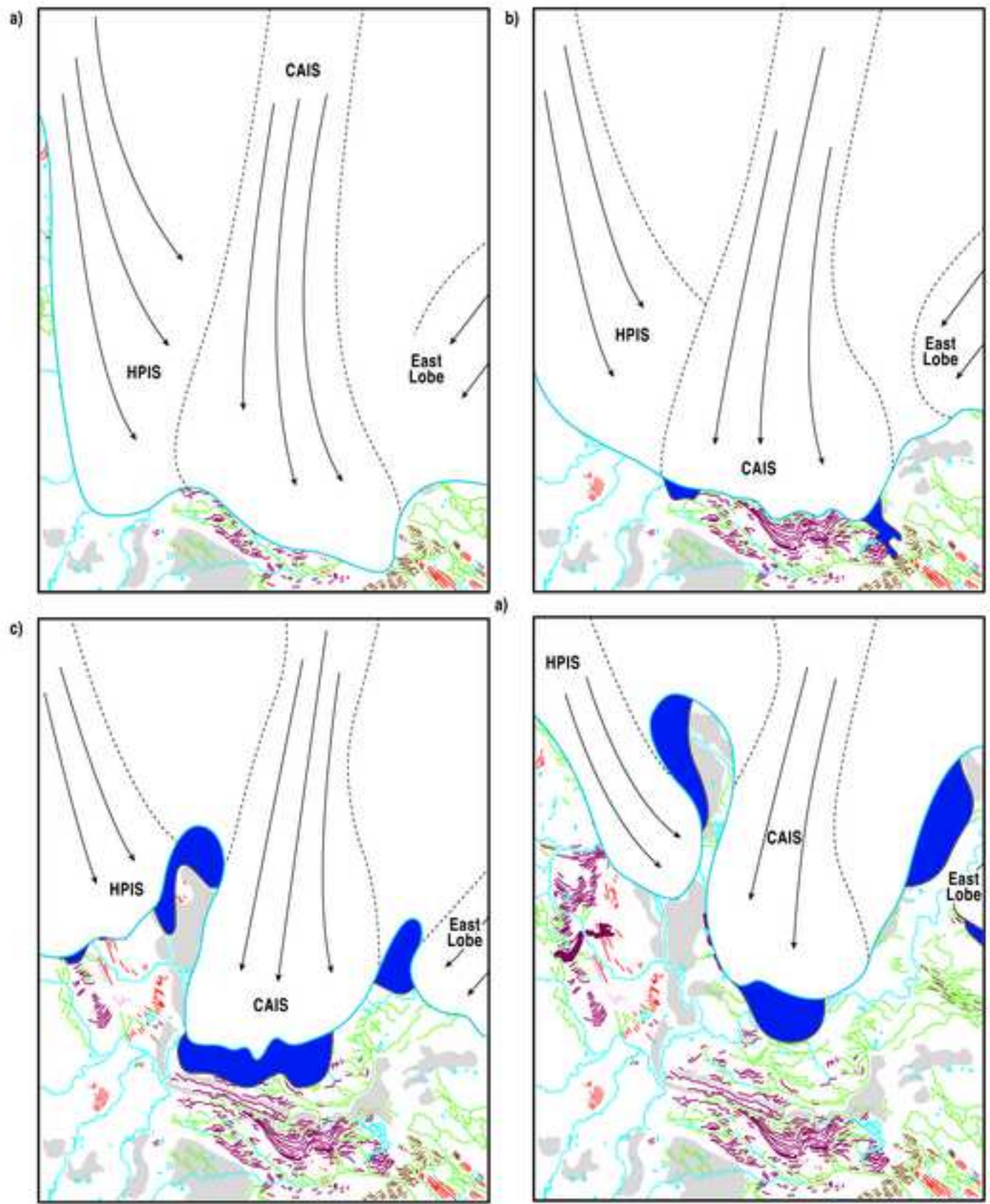


Figure 21a
[Click here to download high resolution image](#)



Figure 21b
[Click here to download high resolution image](#)

